IMPERIAL COLLEGE LONDON

Department of Earth Science and Engineering

Centre for Petroleum Studies

Pierce Field-Improved Oil Recovery by Water Flood Optimisation in a Turbidite Reservoir

By

Despoina Mylonaki

A report submitted in partial fulfillment of the requirements for the MSc and/or the DIC

September 2012

DECLARATION OF OWN WORK

I declare that this thesis

Pierce Field-Improved Oil Recovery by Water Flood Optimisation in a Turbidite Reservoir

is entirely my own work and that where any material could be construed as the work of others, it is fully cited and referenced, and /or with appropriate acknowledgement given.

Signature:

Name of student: Despoina Mylonaki

Name of supervisor: Prof. Peter King

Name of company supervisor: Taco Bieseman

Acknowledgements

I would like to express my sincerest gratitude to Shell U.K. Limited for offering me a scholarship for my studies at Imperial College and for supporting me throughout my research project.

I am most grateful to my supervisor Taco Bieseman for his guidance and help during this study, without which this project would not have been possible. I would also like to thank Dan van Nispen and Shankar Rao, as well as all Shell colleagues for their time and advice.

Gratitude is extended to Prof. Peter King for his overall contribution and to all Imperial College Professors for developing my education the past year.

I will always be grateful to my family and Theodoros for their support and understanding all these years.

Table of Contents

List of Figures

List of Tables

List of Figures- Appendix

List of Tables- Appendix

MSc in Petroleum Engineering 2011-2012

Pierce Field-Improved Oil Recovery by Water Flood Optimisation in a Turbidite Reservoir

Despoina Mylonaki

Prof. Peter King, Imperial College London

Taco Bieseman, Shell U.K. Limited

Abstract

In a complex turbidite field the sweep efficiency of a water flood is dependent on the geological characteristics of the reservoir. In this study the performance of water injection in the Pierce field, a turbidite reservoir in the North Sea that has been developed by gas re-injection and water injection, is investigated and several methods are proposed to improve oil recovery.

Analytical methods were used to understand oil displacement mechanisms in the field and calculate ideal water breakthrough times. Data integration was used to understand the geological properties of the field and the actual behaviour of the water injection. Based on gas production two distinct cases have been identified one with early gas breakthrough and one with late gas breakthrough and aquifer support.

With the use of a field representative sector model water injection performance was modelled and several improvement solutions where tested. The water injection behaviour was demonstrated to be dominated by the highly permeable layers. To evaluate the impact of the main uncertainties on water breakthrough and recovery, sensitivity analysis was performed, which showed that permeability and permeability anisotropy ratio have the highest effect. The recovery factor was found insensitive to the type and the location of the injector due to the absence of horizontal heterogeneity and the existence of the high permeability layers. However, a selective perforation strategy proved to affect the overall oil production, which increases when only the less permeable layers are being perforated.

Two enhanced oil recovery techniques were investigated Water Alternating Gas (WAG) and polymer flooding. WAG injection proved to be beneficial as it decreased the residual oil saturation and hence it increased the recovery factor. The polymer flooding showed similar results as the water injection, without improving sweep efficieny and oil production further. As gas is being injected back into the reservoir WAG can be economically viable and therefore is proposed as an improvement solution to the current water injection strategy.

Introduction

This study investigates how oil recovery from a turbidite reservoir can be improved by optimising water flood in the Pierce field, a turbidite reservoir in the North Sea. The water injection development, which includes three injectors was proved effective for pressure support, but problematic for areal sweep. Two producers watered out due to high water cut and the production stopped. To prevent this from happening to the other two producers the injection rates were decreased significantly. At the moment, the basic reservoir management plan for the field is focusing on reducing the GOR to reduce the decline of the oil rate and maintaining high pressures in the reservoir with low water injection, to improve the displacement efficiency, as this will improve recovery, but also limit the expansion of the gas cap.

The aim of this study is to investigate the performance of the current water injection strategy in Pierce and propose measures for improvement. To understand how the water injection should function, the identification of the ideal displacement is carried out by applying different analycal methods. Extended data analysis is also performed to determine the actual behaviour and compare the results with the ideal one. For testing improvement methods a sector model is created and used for reservoir simulations. The methods tested include improvements of the current water injection strategy but also EOR techniques like WAG and Polymer flooding. As water injection is performed in South Pierce, the study focuses only on this part of the field without taking into consideration North Pierce.

The Pierce field is located 250 km east of Aberdeen in 85m water depth in the North Sea. The field comprises two hydrocarbon accumulations, Pierce North and Pierce South each connected with a salt diaper and both containing an oil column and associated gas caps (Appendix B). The reservoir geology consists of a chanellised turbidite where the Forties sandstone unit is the primary reservoir interval and consists of several sand-shale sequences.

The initial average reservoir pressure in the field is 4650psi in Pierce South and 4825psi in Pierce North at a temperature of 240^{o}F and 255^{o}F respectively. The oil produced is typically a 38^{o}API crude with solution GOR of 1100scf/stb and Formation Vol-

ume Factor of 1.5-1.7 rb/stb. The oil viscosity at bubble point is 0.25-0.3cP.

Development in Pierce began in 1999, as a sub-sea well development with two sub-sea drill centers tied back to the Haewene Brim FPSO (Appendix B). The main production mechanism was depletion drive with gas re-injection due to the absence of a gas evacuation route. As a result of the decline in reservoir pressure, in 2005 water injection was introduced to South Pierce to provide pressure support and sweep. The water injection plan included three producer-injector pairs and a fourth producer was drilled in 2010 (Fig. 1).

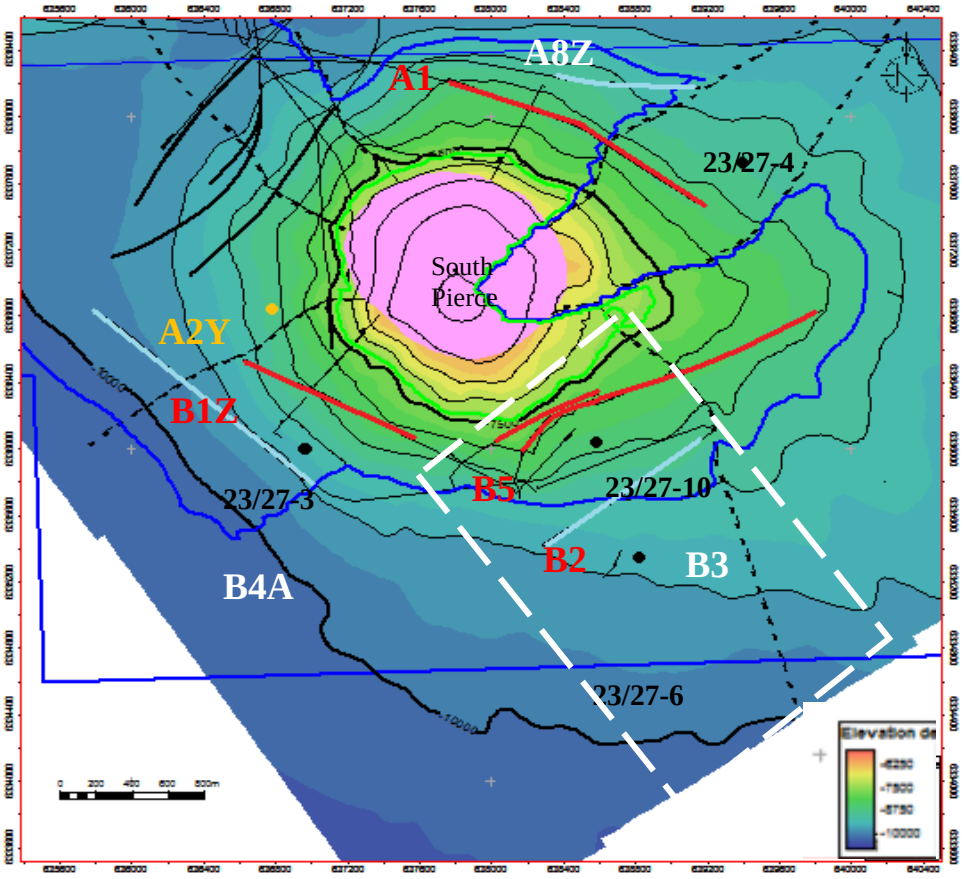

Fig. 1: Map of South Pierce presenting producers (red), water injectors (white), gas injector (yellow), appraisal wells (black) and sector model (white).

Literature Review

The performance of water flooding for increasing the recovery factor has been widely studied throughout the years. The displacement mechanism of oil by water in homogeneous sands has been defined by the fractional flow curve of water (Buckley and Leverett, 1942) and the shock front theory, according to which the shock front saturation occurs at the tangent to the fractional flow (Weldge, 1952). Water flooding efficiency has also been investigated for stratified reservoirs, where flooding occurs first in the high mobility layers (Dykstra and Parson, 1950). Both the Buckley-Leverett and the Dykstra Parsons methods have been used in this study for analytical breakthrough time estimations. Permeability variations perpendicular to the layer have a great effect in recovery, as when permeability increases continuously in an upward direction recovery increases as well, while when permeability decreases upwards lower recovery is obtained (Van Daalen and Van Domselaar, 1972). In the presence of free gas, the residual oil saturations obtained by water flooding are appreciably lower than those obtained in the absence of free gas (Kyte, Stanclift, Stephan and Rapoport, 1956).

New technologies have also been studied, with specific interest in fractured water flood developments across various fields (Van Nispen, Hunt, Hartwijk and Trofimov, 2006). Proposals from this paper regarding the selective perforation strategy have been used in this study. Water injection under fracturing conditions has also been investigated for the Pierce field as the maximum injection rates are restrained by potential dynamic fractures (Hustedt and Snippe, 2010). However, there are other Enhanced Oil Recovery (EOR) techniques that can improve recovery factor, but each one can be used in specific conditions and faces different problems (Farouq and Thomas, 1996).

Methodology and Analysis

The approach taken to understand the current water injection strategy and propose measures for improvement consists of four parts:

- Determination of ideal displacement behaviour using analytical tools
- Review of reservoir and well data for the evaluation of the actual displacement behaviour
- Evaluation of the displacement behaviour using numerical simulation
- Improvement solutions

Ideal Displacement Behaviour

For the identification of the ideal displacement behaviour of the reservoir two analytical methods were used to calculate the water breakthrough time, the Buckley and Leverett analysis and the Dykstra and Parson method as proposed by Dake (1978, 1994).

Buckley-Leverett Analysis (BL). This method describes immiscible displacement in one dimension in homogeneous reservoirs for diffuse flow. Based on the fractional flow curve and the shock front theory, the method provides the water breakthrough time and the recovery factor. (Appendix C)

Data for the application of the BL method were obtained from two appraisal wells, which were selected according to their location, 23/27-10 which is near producers B1Z, B2 and B5 and 23/27-4 which is near producer A1. The SCAL (Special Core Analysis) data from the appraisal wells were studied in order to obtain the variation of oil and water relative permeability to water saturation. Oil and water viscosities for each well were obtained from the PVT (Pressure Volume Temperature) data of the producers. The fractional flow equation neglecting capillary pressure and gravity segregation is:

$$f_w = \frac{1}{1+\frac{\mu_w \, k_{ro}}{k_{rw} \, \mu_o}} \tag{1}$$

After calculating and plotting the fractional flow curves (Fig. 2), the breakthrough was estimated at $S_{w,bt}$= 0.651, f_w= 0.852 for well 23/27-4 and $S_{w,bt}$= 0.506, f_w= 0.893 for well 23/27-10 and the breakthrough time, which for a constant rate of water injection is related to the dimensionless water influx was calculated by the expression

$$t = \frac{W_{id} * h_{res} * \phi * d_{inj} * d_{inj,prod}}{q_i * 5.615 * 365} \text{ (years)} \tag{2}$$

where,

$$W_{id} = \frac{1}{\frac{df_w}{dS_w}} \tag{3}$$

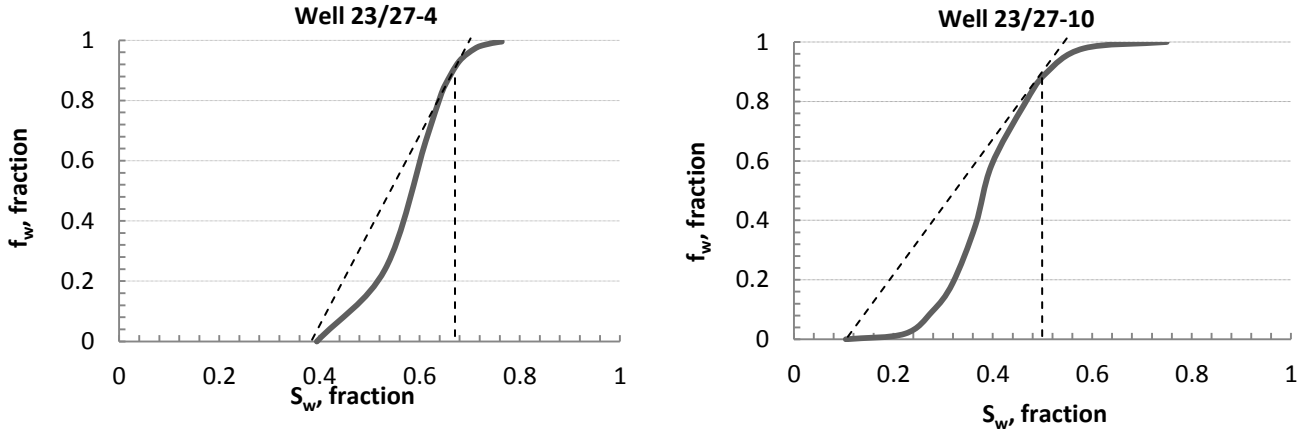

Fig. 2: Fractional flow curve for two different appraisal wells.

Using the fractional flow curves of the appraisal wells the breakthrough time was calculated for each producer and injector pair by applying different injection rates and distances (between injectors and injectors-producers), as presented in Table 1, and for all the SCAL samples available. These values represent the actual distances between the wells in the field and also the actual injection

rates. The final breakthrough time for pair A1-A8Z was estimated at 6 years, for pair B1Z-B4A at 17.7 years and for B2-B3 and B5-B3 which showed the same breakthrough time at 13 years. The difference in the breakthrough time between A1, B1Z, B2 and B5 can be mainly attributed to the thickness of the reservoir and the distance between the injector and the producer.

Parameter	Wells		
	A1-A8Z	B1Z-B4A	B2, B5 – B3
h_{res} (ft)	400	590	525
d_{inj} (ft)	5000	5000	5000
$d_{inj,\ prod}$ (ft)	720	1050	1620
q_i (bbl/day)	6000	5000	10000

Table 1: Parameters used for the calculation of breakthrough time.

Dykstra-Parsons Analysis (DP). This method describes the displacement of fluids in stratified reservoirs and can calculate vertical sweep efficiency for all values of the mobility ratio, M (Appendix D). For this method the reservoir is assumed to be divided into layers with the same permeability across the whole layer and the fractional flow is calculated, according to the order in which the layers flood, neglecting gravity segregation and cross flow, by the expression

$$f_w = \frac{\sum_{i=1}^{n} \frac{\lambda_i h_i}{A+1}}{\sum_{i=1}^{N} \frac{\lambda_i h_i}{Ax_i+1}} \tag{4}$$

Three appraisal wells were selected 23/27-4 near producer A1, 23/27-6 near B2, B5 and 23/27-3 near B1Z. From the log data, the layering of the reservoir and the corresponding permeabilities were obtained in order to calculate the fractional flow curves (Fig. 3).

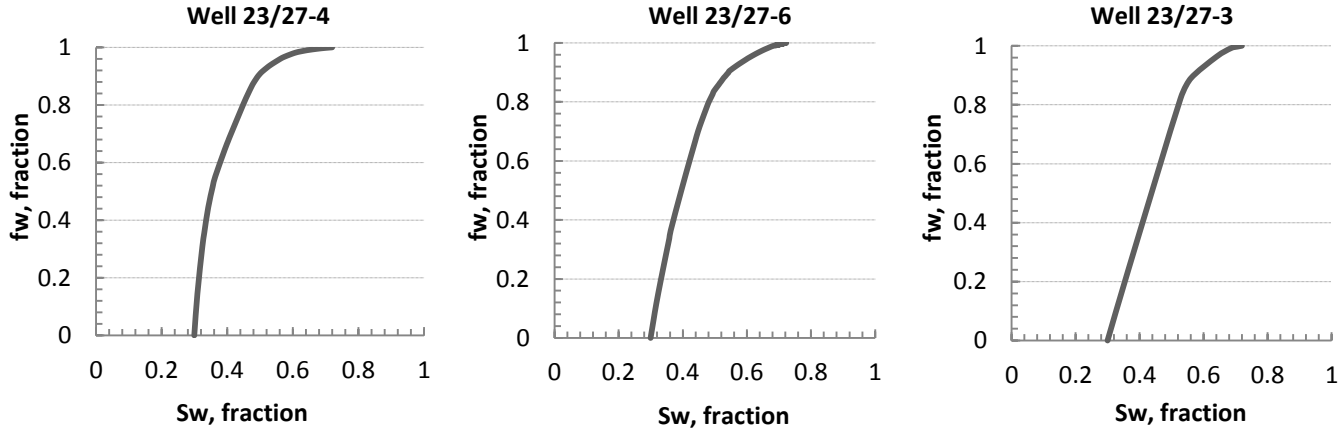

Fig. 3: Fractional flow curves for the three appraisal wells.

After the calculation of the fractional flow the breakthrough time was calculated using Eq. 2 and Eq. 3 and the same injection rates and distances were used (Table 1) in order for the results to be comparable with the Buckley-Leverett method. For pair A1-A8Z the breakthrough time was estimated at 0.56 years, for pair B2-B3 and B5-B3 at 0.67 years and for B1Z-B4A at 3.5 years.

Comparison of BL and DP. By comparing the results from the two methods different breakthrough times can be observed. The BL method gives higher breakthrough times, as it assumes that the reservoir is homogeneous. In this case the whole thickness of 500 ft must be flooded before the water from the injector reaches the producer. Also, in this theoretical approach capillary and gravitational effects are neglected, but these effects are present in the reservoir. Gravitational forces tend to promote complete vertical segregation of oil , gas and water and capillary forces tend to oppose to the formation of saturation discontinuities. The DP method gives lower breakthrough time due to the layering. Water moves through the layers with higher permeabilities and reaches the producer faster, as no cross flow between the layers is assumed. In this method, gravity segregation is also neglected as in the BL and pressure drop across each of the layers is assumed constant. However in reservoirs which have been depleted prior to water injection like Pierce, there will be differential depletion between the layers, with those of high flow capacity having the lower pressures.

Integrated Review of Reservoir and Well Data

In order to understand and improve the performance of the water injection strategy after identifying the ideal behaviour all the available data were analyzed and evaluated, including geological data, production and injection rates, pressures from downhole gauges, water tracer measurements and 4D data. These data were also used in order to understand the key uncertainties regarding the geology of the field.

Field Geology.The geology of the field is highly complex due to the turbidite nature of the reservoir. The presence of the salt domes, which obstruct the seismic imaging results in uncertainty in the structural interpretation. Also, due to the salt domes the reservoir has a dip of 45-60^{o}. The average porosity is estimated at 17% and the permeability varies from 0.01 to 300mD with individual high permeability layers and shale layers of unknown length and continuity. Due to its variation permeability represents together with the permeability anisotropy ratio (k_v/k_h) the main uncertainties of the field affecting flow. In the south side of South Pierce, where well B2 is located, a small aquifer is present, while in the west and east side of the salt dome no aquifer support is observed. Important parameter of the field is also the tilting of the Oil Water Contacts (OWC) according to which different OWC are identified across the field (Dennis, Baillie, Holt and Wessel-Berg, 2007), but this aspect is not considered in this study.

Production-Injection Rates. Although an extended production test was performed in 1996, well B1Z started producing on March 1999 with an oil rate of around 8,000 bbl/d and gas rate of 30-40MMscf/d (Fig. 4). Water injection started in December 2004 from injector B4A with a positive effect on the production. In May 2007 water broke through and the well started producing oil and water with a low water cut of 30-40% (Fig. 5). Production from well A1 started also on February 1999 with an oil rate of around 4,000 bbl/d and gas rate of 6MMscf/d (Fig. 6). Water injection started in December 2005 from injector A8Z, but high injection rates caused fracturing of the reservoir and water cut increased rapidly, the well water out very quickly and production stopped in August 2006 (Fig. 7). Well B2 started producing on February 1999 with an oil rate of around 10,000 bbl/d and gas rate of 15-20MMscf/d (Fig. 8). In May 2001 the well started producing water with increasing water cut from 1 to 20%, due to the small aquifer present at the area .Water injection from well B3 started in April 2005, when the water cut started increasing further and in August 2008 the well watered out and production stopped (Fig. 9). Although well B5 is near B2 it behaves differently. Production started on November 2010 and continues with 0% water cut, while water is being injected from B3 (Fig. 10). From the gas production and the water cut two different behaviours are observed across the field. In well B1Z high gas rates are observed which indicate early breakthrough from gas injector A2Y, but this behaviour is not observed in wells A1 and B2 as gas production is lower. Also, the aquifer presence is only observed in well B2.

From the production and injection rates the water breakthrough time was estimated at 2 years and 6 months for well B1Z, 6 months for well A8Z and B2, while well B5 is still producing with 0% water cut. The breakthrough times from the data show a similarity to the DP results, but not to the BL values, which indicates that the DP method is more appropriate for predicting the behaviour of the water injection in Pierce.

Pressure Data. Communication between the injectors and the producers is verified by the available datum pressure data (downhole gauge pressures). As production starts pressure depletion is observed, but as soon as injection begins a quick response, after 6 months, in the pressure is observed for producers A1 and B2, with the pressure increasing (Fig. 6, Fig. 8). For producer B1Z (Fig. 4) the pressure response is not observed immediately, but after 2.5 years, indicating that there might be a barrier or a baffle between the wells blocking direct flow. Also, from pressure data, communication between producer A1 and B2 is identified, as these wells have similar pressure profiles (Fig. 6, Fig. 8). From the pressure data generally it can be verified that water injection is successful in providing pressure support (Appendix E).

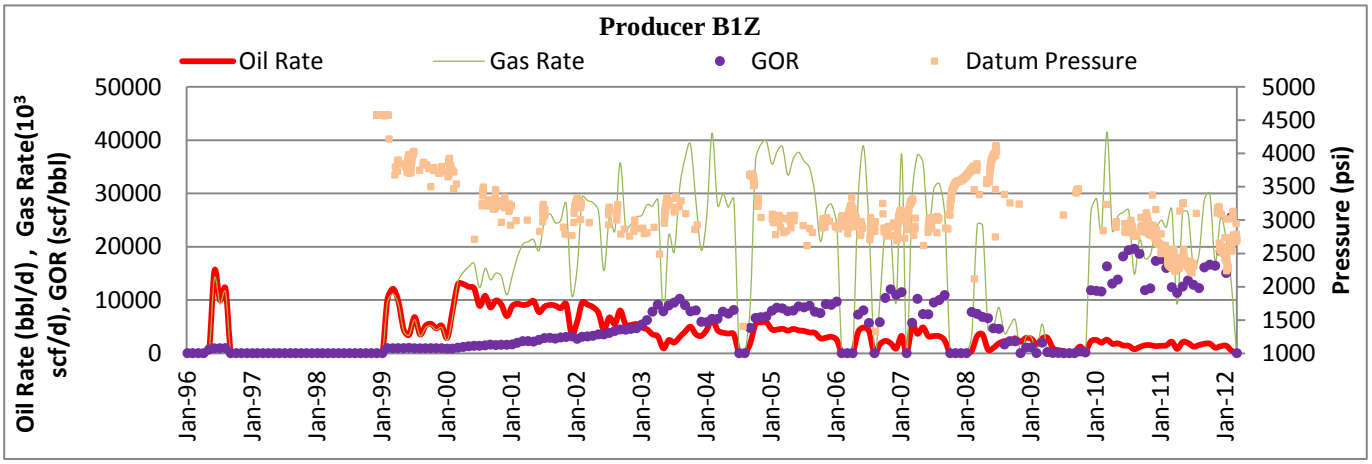

Fig. 4: Production data for producer B1Z.

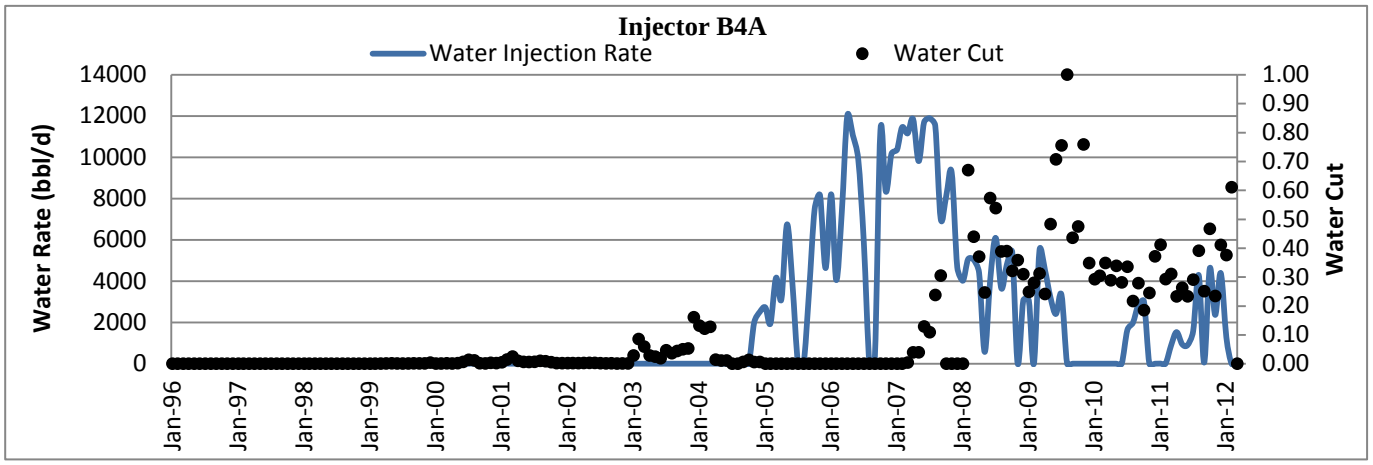

Fig. 5: injection data from injector B4A.

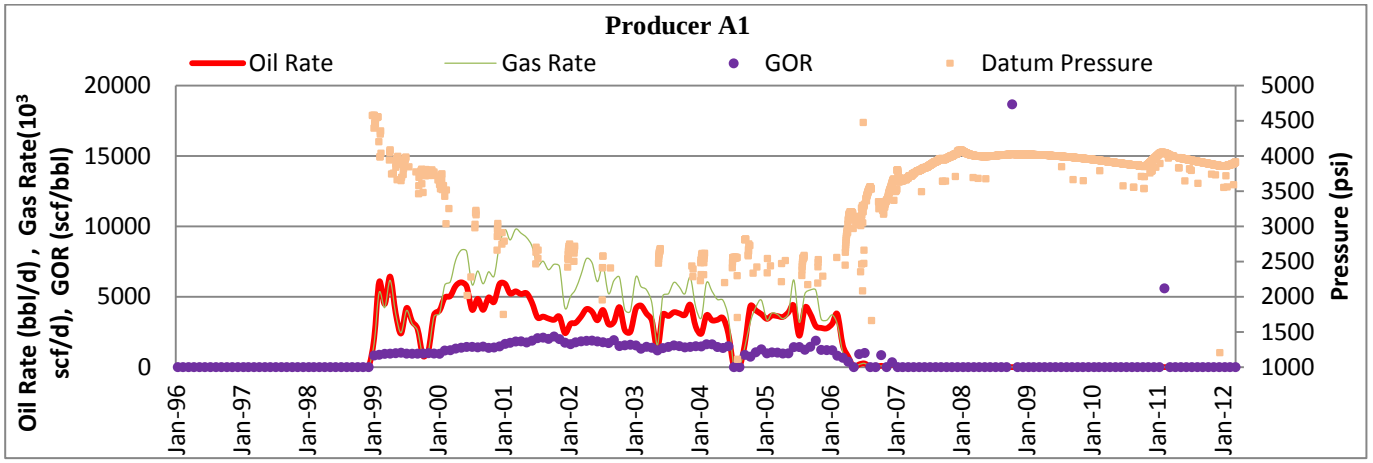

Fig. 6: Production data from producer A1.

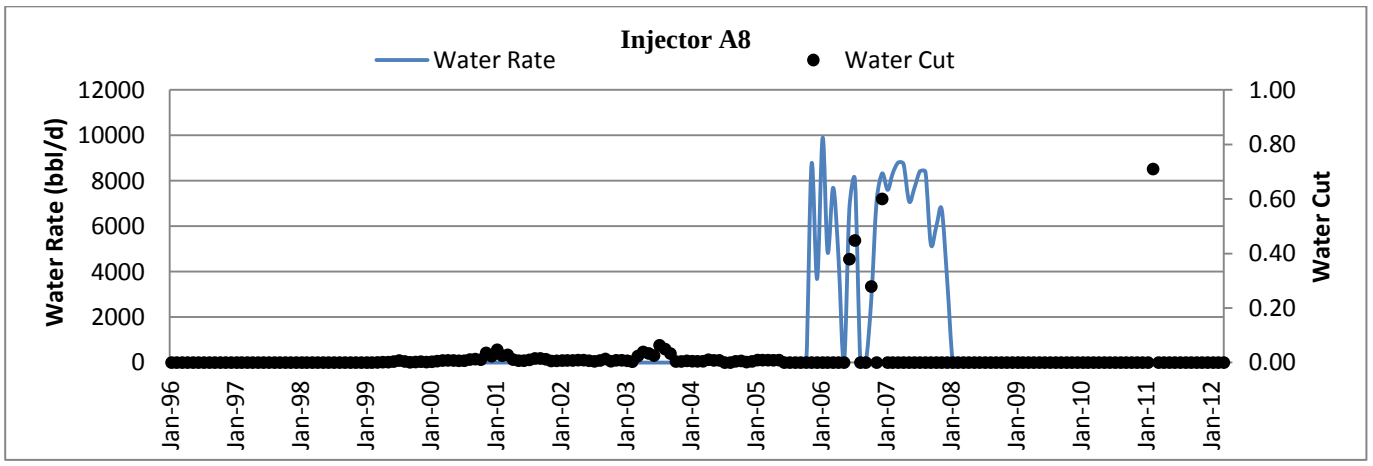

Fig. 7: Injection data from injector A8Z.

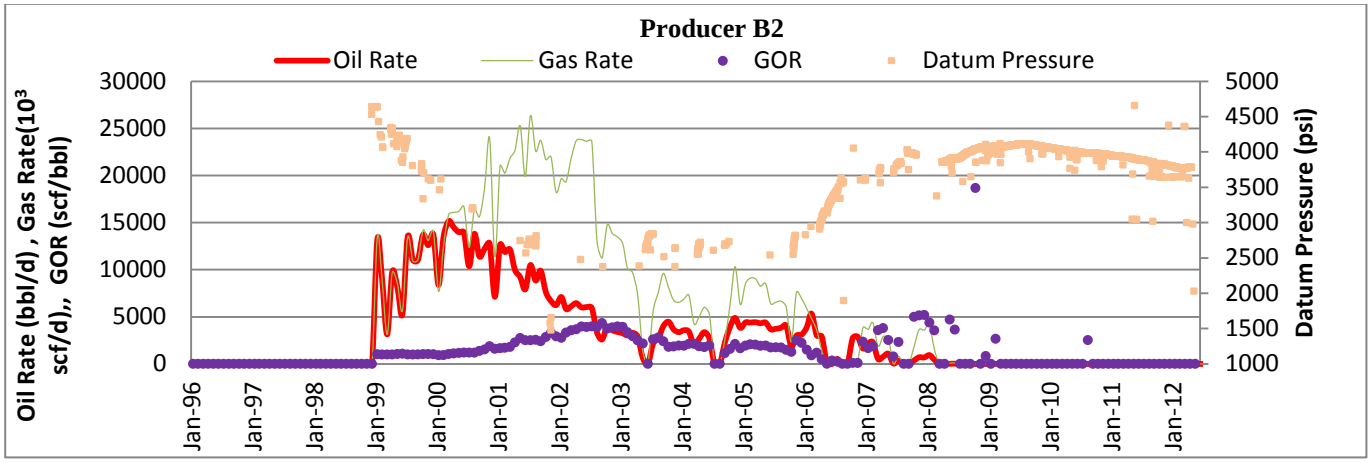

Fig. 8: Production data from producer B2.

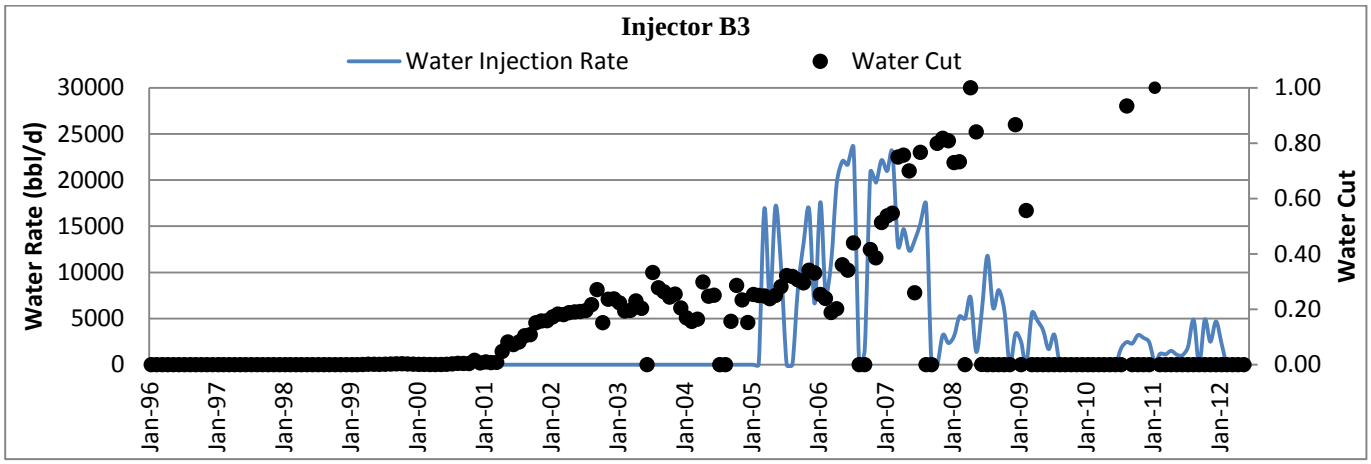

Fig. 9: Injection data for injector B3.

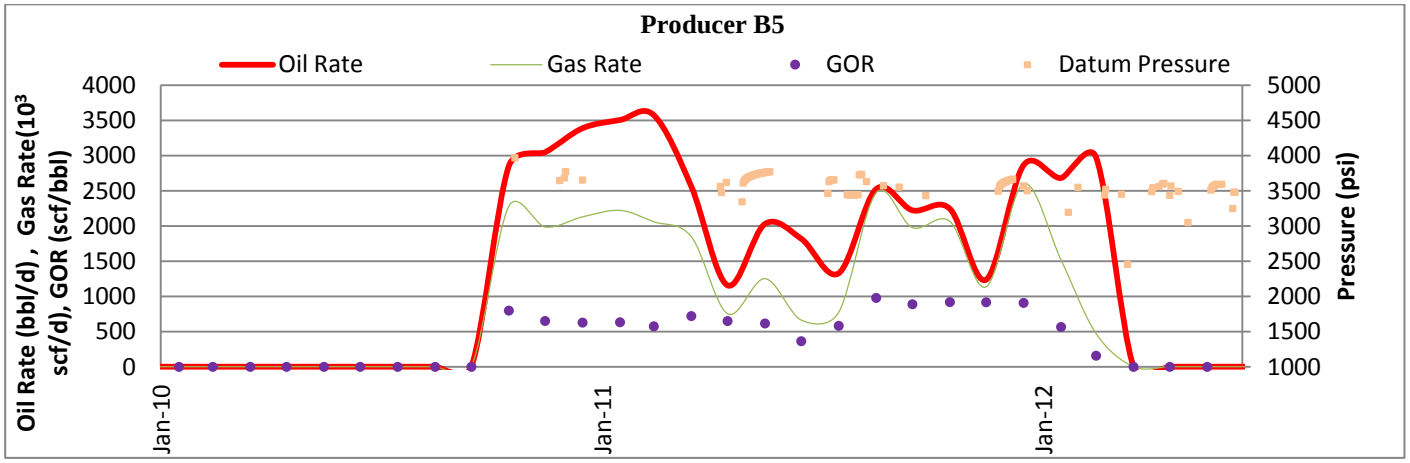

Fig. 10: Production data for producer B5.

Water Tracer Data. Tracer experiments were performed in order to further investigate the communication between the injectors and producers. Aqueous solutions of T158a, T158c and T140c were injected from wells A8Z, B4A and B3 respectively. Water samples were taken from producers A1, B2 and B1Z and their analysis gave the following results (Appendix F):

- Tracer T158a injected in A8Z was detected in A1, B2 and B1Z
- Tracers T158c and T40a injected in B4A was not detected in any of the producers

- Tracer T140c injected in B3 was detected in B1Z

Tracers from A8Z detected in producers A1 and B2 indicate communication between the wells, which is consistent with the observations made from the pressure data. However the detection of A8Z tracers in B1Z is quite ambiguous, since this well is located on the west side of the salt diapir and water needs to travel more than 2km to reach it. Contamination should also be considered since B1Z and B2 share the same flowline. Tracers from B4A were never detected by an oil producer, although from production data communication between B1Z and B4A is identified. The reason might be the time of sampling, which could not have been enough for the producer to pick up the tracer or maybe the presence of a baffle or a barrier. Tracers from B3 were observed in B1Z, but not in B2, which could also be due to a baffle or a barrier.

4D Seismic Data. In 2009 4D seismic data were acquired. The map (Fig. 11) presents 4D amplitude and significant information is provided for wells B1Z-B4A and B2-B3. In injector B4A an increase of pressure (red area) is observed due to water injection and also a hardening signal (blue area) which indicates sweep at the end of the producer. The pressure signal is very high in the red area indicating that pressure support is not distributed across the entire area, but only in this small region. This behaviour could be due to a baffle or barrier constraining pressure, as observed from the tracer data. This observation can also explain why the breakthrough time in B1Z is only after 2.5 years. The same signals are observed in B2-B3, but for this pair the sweep takes place at the centre of the producer, which also verifies with certainty the communication between the wells. Here the pressure signal shows a better distribution between the injector and producer, as no red signal is observed.

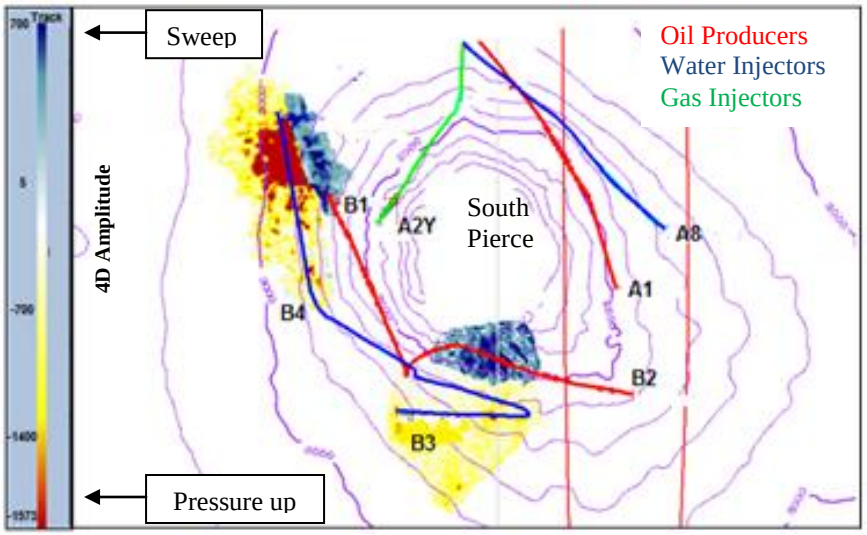

Fig. 11: Map of 4D amplitude signals, showing pressure increase and sweep.

Field Representative Sector Model

To investigate the effect of reservoir heterogeneity and the impact of the main uncertainties on sweep efficiency a reservoir simulation model was constructed using the in-house simulator MoRes. This model was also used to determine the benefits of EOR techniques like WAG and polymer flooding.

Sector Model. The model is a tilted box model representing a producer injector pair of the field. The size of the model was chosen at 1.5x2km with a reservoir thickness of 152m and 30x40x60 (XYZ direction) grid blocks. The height of each layer was chosen at 2.5m. The reservoir dip was set at 45^{o} and the OWC and Gas Oil Contact (GOC) at 3078m and 2271m respectively (Fig. 12a). Input porosity was set at 17% and Net To Gross (NTG) was multiplied with a factor of 0.65 to represent the significant amount of shale bodies into the reservoir. The model was populated with a permeability profile based on well logs. From the logs, according to permeability and porosity different layers were identified and by taking the average permeability for each layer, a single value of horizontal permeability, between 0.01 and 300mD, was assigned across each layer (Fig. 12b) The initial k_v/k_h ratio was set at 0.001, as this value was considered the most representative for the field. For the fluid properties a black oil model was selected and the values were assigned according to the PVT data from the appraisal wells. For the relative permeability data including end point permeabilities and Corey parameters the same SCAL data were used as in the BL. In the sector model three wells were modelled a producer, a gas injector and a water injector.

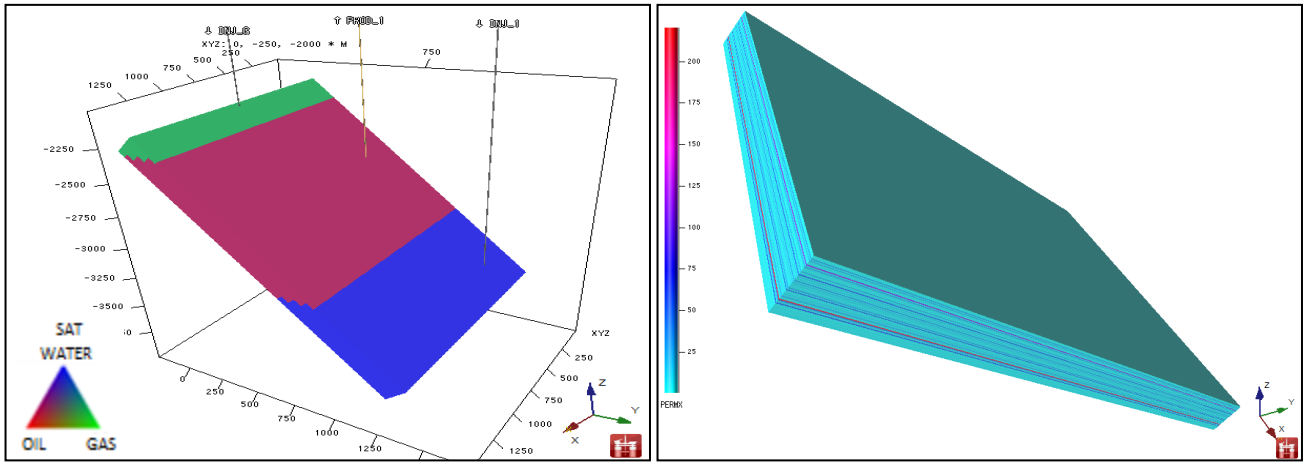

Fig. 12: (a) Saturation in sector model, (b) Horizontal permeability in sector model.

Base Case (BC). The base case comprise a gas injector, a producer and a water injector. The vertical gas injector was placed at the top of the structure in the GOC to re-inject the produced gas. A deviated producer, crossing more than twenty layers, was chosen and placed in the middle of the oil column. Due to the maximum gas volume the FPSO can handle, all producers in the field are gas constrained, hence a 25MMscf/day constraint was applied to the producer, as well as a minimum Bottomhole Pressure (BHP) of 1500 psi. The water injector was also modelled deviated with a maximum water injection rate of 2500bbl/day to represent the current low injection strategy and with a maximum BHP of 6000psi. The entire deviated part was perforated and the simulation time was set at 30 years, with water injection starting after 6 years. The first 6 years represent the period during which the field was developed under pressure depletion (Appendix G).

From Fig. 13 it is observed that flow starts initially from the high permeability layers, as gas flows quickly from these layers into the producer (1 year) and early breakthrough occurs. For water, flow similarly starts from these highly permeable layers, but due to the pressure from the gas cap it initially flows much slower (1 year). Actual water breakthrough occurs after water injection starts (6 years). By comparing and combining the results from the analytical and the simulation models it has been observed that the flow behaviour is dominated by the layering of the reservoir and specifically the high permeability layers. The DP method can give good estimation of the breakthrough time as the results match those obtained from the simulation, while the BL results vary significantly.

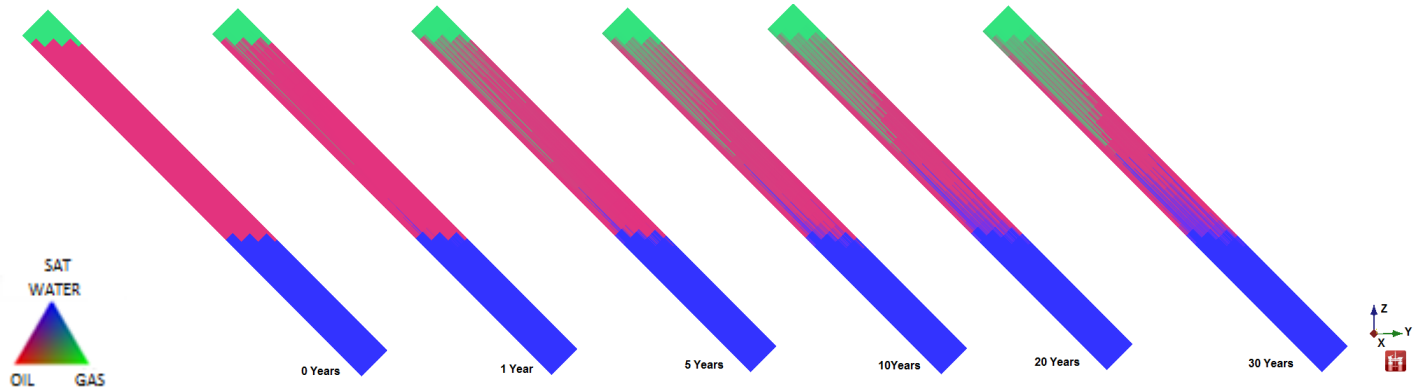

Fig. 13: Cross section of saturation in the ZY direction for 6 time steps of the simulation for the BC.

Base Case Gas Cap Constrained (BC-GCC). The behaviour of the BC represents the performance of producer B1Z, but not B2. Therefore, a second approach was investigated in order to model a case with low aquifer support and delayed gas breakthrough. To achieve this, horizontal permeabilities in the gas cap grid blocks were multiplied by a factor of 0.001 in order to constrain the high permeability layers. From comparing the results for the two cases (Fig. 14a) it can be observed that for the BC-GCC gas breakthrough is, as expected, not observed in year 1 (Appendix H) .This delay results in an increase in oil production. Water cut occurs earlier and higher values are observed during the simulation. In both cases, after year 6, when water injection starts there is a rapid increase in water cut with values not higher that 60%. The cumulative oil production (Fig. 14b) is 30.66 MMbbl for the BC-GCC and 26.94MMbbl for the BC, so the recovery factor increases from 34% to 39%.

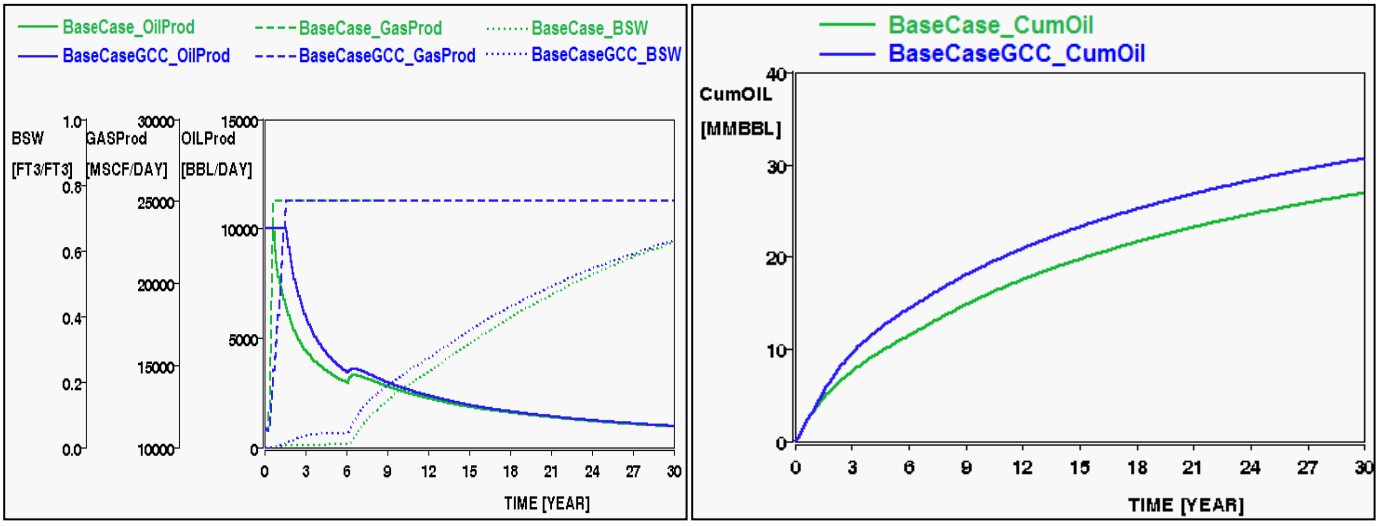

Fig. 14: For the Base Case and the Base Case GCC profiles of (a) Oil production, gas production and water cut, (b) Cumulative oil production.

Sensitivity Analysis. Several sensitivity cases were run to cover a range of uncertainties in the parameters, which have high impact on recovery. The permeability, the k_v/k_h ratio and the relative permeability data, including Corey parameters and end point relative permeabilities, are the main uncertainties and as the sector was not obtained from a static model, but created according to the overall field properties, the uncertainty around these parameters in the sector increases even more. Grid block size can also impact the results of the simulation. The sensitivity of water cut and cumulative oil production to relative permeability data, the k_v/k_h ratio, permeability and grid block size was investigated. For permeability two different cases were modelled one with permeability of higher contrast (lower permeability for less permeable layers and higher for highly permeable layers) and one of a homogeneous reservoir.

The results illustrate (Fig. 15) that the impact of k_{rw}, $N_{w,}$ N_o and grid block size on water cut is minor, with only the shape exhibiting some sensitivity. For N_o, although at the beginning of the water injection a higher value of N_o gives lower water cut, at the end the reverse behaviour is observed. S_{wc} and S_{or} influence water cut more, with a ±0.05 difference at each case. However, the variables affecting water cut the most are permeability and k_v/k_h ratio. The lower the k_v/k_h the higher the water cut, because with lower vertical permeability water moves faster (horizontally) towards the producer instead of flowing through other layers, resulting in higher water production. This is also justified by the permeability sensitivity. In the homogeneous case the water front movement is more uniform and water cut is lower, while in the case with higher contrast water cut increases more than 0.15. The cumulative oil production (Appendix I) is also insensitive to k_{rw}, $N_{w,}$ N_o and grid block size and for S_{wc} and S_{or} a small impact is observed. Cumulative oil production is highly sensitive to permeability and k_v/k_h. Higher values of the permeability anisotropy ratio result in higher oil production, because with higher vertical permeability, water floods and flows through all layers achieving better sweep efficiency and lower water production. Identical results are observed for the homogeneous case.

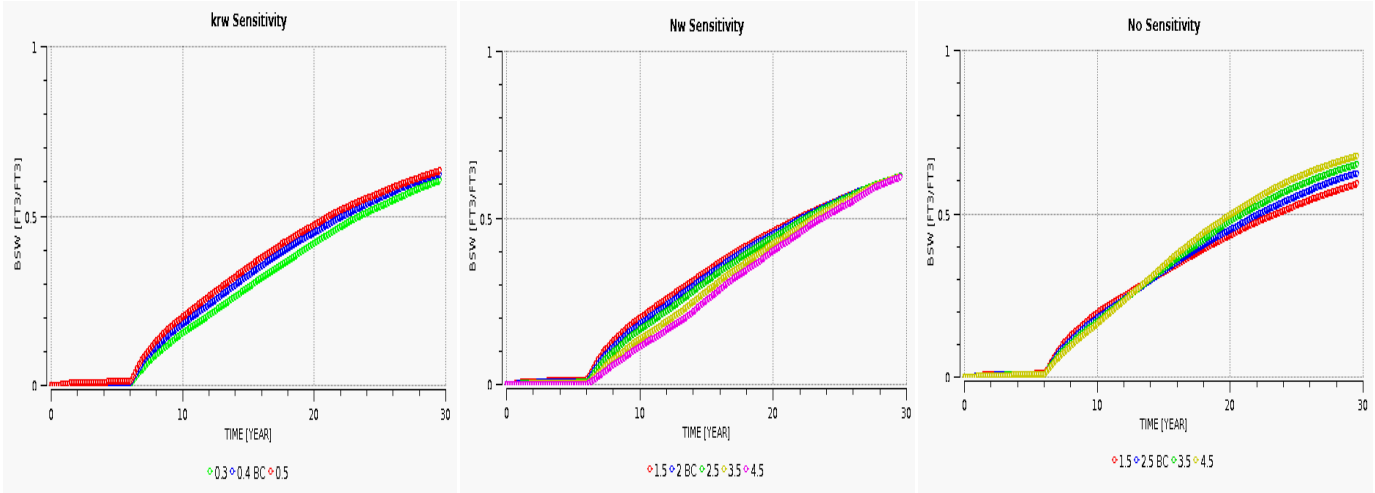

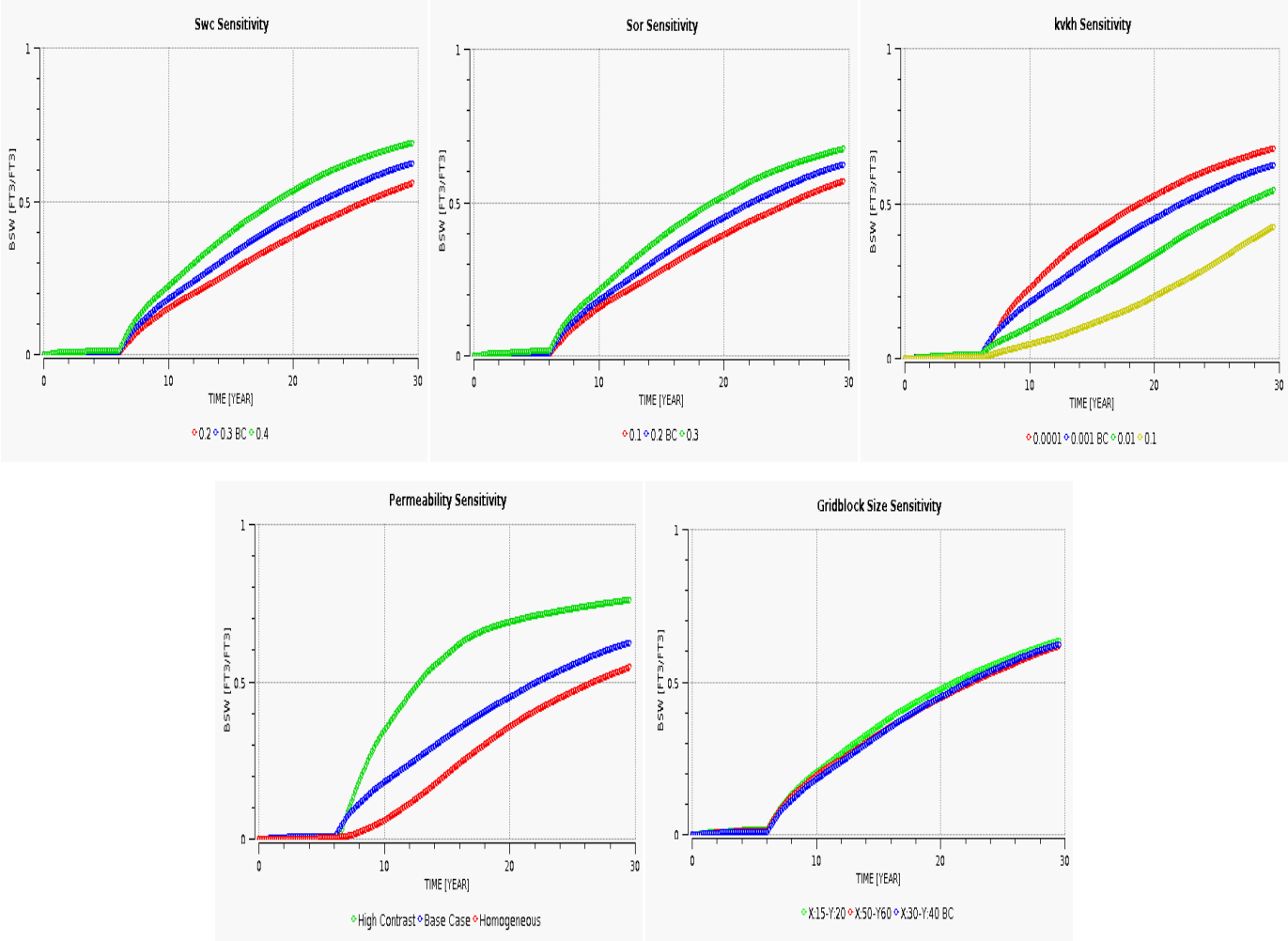

Fig. 15: Sensitivity of water cut to relative permeability parameters, permeability, k_v/k_h ratio and grid block size.

Proposals to Improve Water Flood Efficiency

To improve the efficiency of the water flood several improvement solutions were tested. Clearly, increasing to a recovery factor of 34% or 39% is not an easy task and rapid or significant changes cannot be expected, but by applying different solutions a better understanding of the field is also achieved. As a new water injector is planned to be drilled in the next 2 years different alterations were tested using the current injection strategy in order to maximize its performance. The performance of WAG and Polymer Flooding was also investigated for later application in the field.

Water Injection. For the BC and the BG-GCC different sensitivities were performed regarding, the type of the injector, the location, the perforations and the injection rate.

Well Type. Instead of a deviated well the performance of a vertical and a horizontal well were also investigated. The vertical well was located in the middle of the water column and perforated through all layers. From the results no difference in the breakthrough time and the final recovery was observed compared to the deviated well, which crosses only 45 layers. The reason is that the deviated well does not cross the 10 upper and 5 bottom layers which have significantly low permeability and hence do not affect flow. Another observation made is that in both cases the flow behaviour is dominated by the highly permeable layers and the k_v/k_h ratio, which is not 0 and therefore no difference is observed when using the vertical well.

The horizontal well was placed in the same location as the deviated, but the horizontal section crossed only 12 layers. As a result, the breakthrough time and water cut remained the same (as these parameters are affected by the high permeability layers), but the recovery factor decreased 2% and 3.5% for the BC-GCC and the BC respectively, because the sweep efficiency decreases as parts of the reservoir remain unswept with the horizontal well (Appendix J).

Well Location. The position of the injector in the BC is in the middle of the water column, so two different cases were modelled one with the injector near the OWC (top of the water column) and one with the injector at the bottom of the aquifer. For both cases no significant changes were observed regarding both the breakthrough time and the oil production. As soon as water injection

starts, irrespectively of the position of the injector, due to the highly permeable layers water moves with the same speed and reaches the producer at the same time. This insensitivity of the oil production to the well location is due to the absence of horizontal heterogeneity.

Perforations. As stated above, the flow behaviour in the model is particularly affected by the high permeability layers. In the initial cases, the whole horizontal section of the injector was perforated, resulting in the majority of water flowing only through these highly permeable layers. To eliminate this phenomenon a selective perforation strategy was performed, in which only the low permeability layers were perforated to force water flow through them (Van Nispen, Hunt, Hartwijk and Trofimov, 2006). As a result in both the BC and the BC-GCC a 1% increase in the recovery factor is observed and 0.1 decrease in water cut, as less water is produced (Appendix J). Water still flows from the highly permeable layers, but with this strategy higher sweep is achieved in the less permeable layers.

Injection Rates. Fracturing of the reservoir was caused after injecting more than 10000bbl/day of water from well A8Z and as a result after that a low injection strategy was established. A sensitivity analysis for the BC was performed regarding injection rates, without taking into account the fracturing nature of the reservoir, to investigate sweep efficiency for 1500bbl/day, 2500bbl/day, 3500bbl/day, 4500bbl/day, 5500bbl/day and 6500bbl/day. From the results (Fig. 16) it is observed that as expected the average datum pressure increases for higher injection rates and the breakthrough time is the same but higher water cut is observed with values of 0.8 and 0.9 for 4500 and 5500bbl/day. So, although better pressure support is achieved, due to the increase in water production the cumulative volumes of oil produced are almost similar, indicating that water is being circulated through the highly permeable layers and better sweep is not achieved. Therefore, the current low injection strategy with 2500bbl/day is identified as the most appropriate with a potential increase till 4000bbl/day, however before higher rates can be applied consideration must be given to the possibility of fracturing the reservoir.

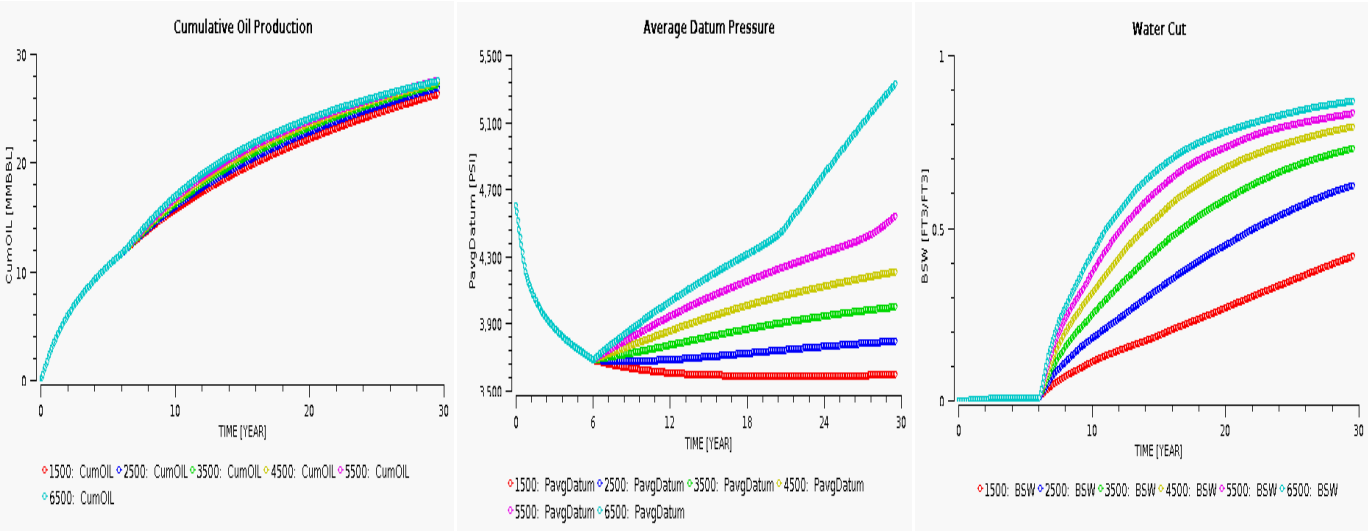

Fig. 16: Sensitivity of (a) cumulative oil production, (b) average datum pressure and (c) water cut to water injection rates.

Water Alternating Gas (WAG). The injection of water with gas in alternating slugs is known for improving sweep efficiency based on changes in the mobility contrasts. Water injection keeps the reservoir pressure level high, which is necessary for gas to achieve miscibility, increase additional gas storage and decrease the oil viscosity. Because of gravity segregation, the injected gas and water tend to sweep different portions of the pore space. Generally, gas invades the upper portions of the reservoir while the water invades the lower portion (Wu, Ogbe, Zhu and Khataniar, 2004).

Since the produced gas is re-injected in the field this option is potentially economically viable and therefore modelled to investigate its efficiency. The WAG injection was not performed simultaneously, with gas and water being injected at the same time, but alternating every 6 months. Differenet injection rates were tested for both water and gas slugs and the optimum rates giving higher recovery factors were identified at 4000bbl/day of water and 25MMscf/day of gas. As the production is gas constrained at 25MMscf/day, when the WAG injector injects gas the gas injector at the gas cap remains inactive for the 6 month period after which injection starts again.

The results illustrate that with the WAG injection a 2-2.5% increase in recovery factor for both cases. As gas is injected into the reservoir the oil production increases and the average datum pressure decreases, but when water injection starts the opposite behaviour is observed and the pressure increases (Fig. 17). During the gas injection, water is pushed into the producer and the water production increases resulting in higher water cut values during the simulation, but with a final value of 0.6.

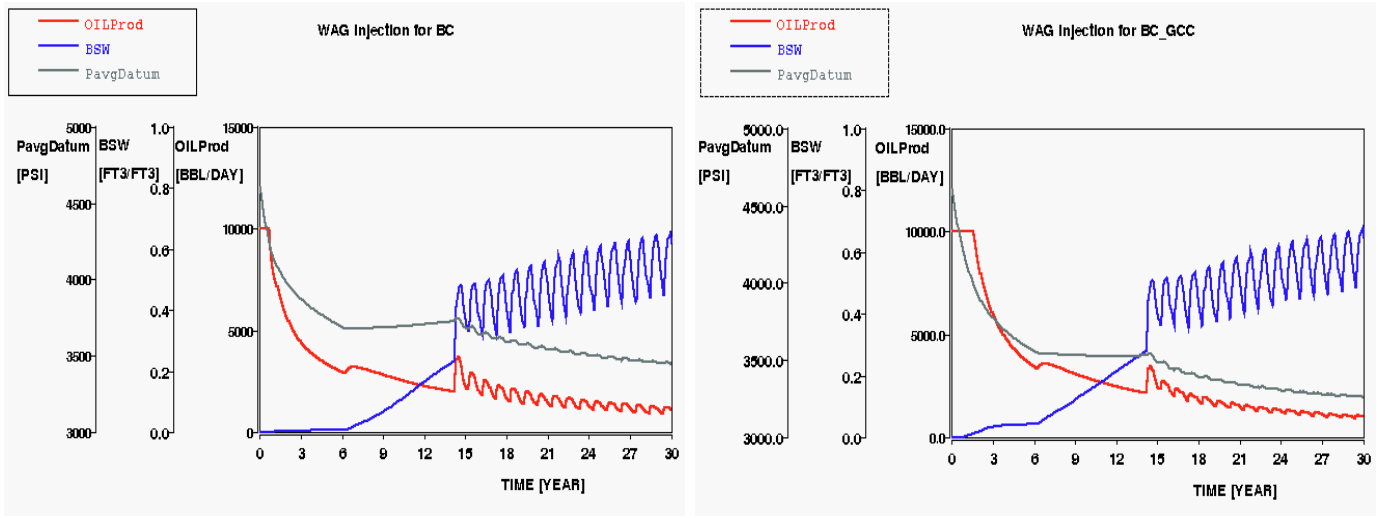

Fig. 17: Oil production, water cut and average datum pressure profiles for BC and BC-GCC for the WAG injection.

The BHP in the producer as soon as gas is injected starts decreasing and increases for water injection (Appendix J). For both cases the BHP constraint of 6000psi is never reached, but the gas injector pressure is very close indicating that further gas cannot be injected. For the water injector as the BHP is below the constraint higher injection rates were tested and gave higher oil recovery (but still fracturing has to be considered).

Although, the WAG process is supposed to sweep both the bottom and the top of the reservoir, due to the layering and specifically the highly permeable layers this behaviour is not observed. On the contrary, both phases flow through the same layers. After water flooding, a specific residual oil has remained into the pore space and as illustrated in Fig. 18 as gas is injected after the water injection this residual oil is being swept increasing the final recovery.

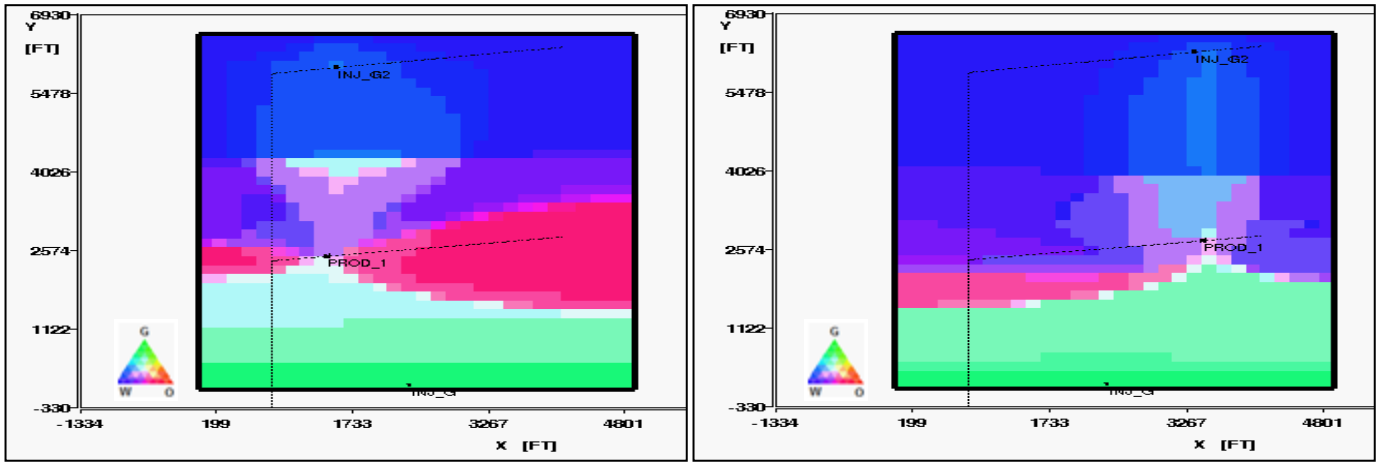

Fig. 18: Saturation profiles of BC for two highly permeable layers, illustrating sweep efficiency of WAG at year 20.

Polymer Flooding. Polymer flooding consists of adding polymer to the water of a water flood to decrease its mobility. The resulting increase in viscosity, as well as a decrease in aqueous phase permeability that occurs with some polymers, causes a lower mobility ratio. This lowering increases the efficiency of the water flood through greater volumetric sweep efficiency and a lower swept zone oil saturation. The greater recovery efficiency constitutes the economic incentive for polymer flooding when applicable (Lake, 1996).

The water viscosity in the model is lower than the oil and hence polymer flooding was investigated in order to decrease the mobility ratio. For modelling and simplicity purposes instead of adding a fourth phase representing the polymer, the water viscosity was increased after a certain time step.

The results illustrate that with the polymer flooding a 0.5% increase in the cumulative oil production is achieved. By the time the polymer is added the BHP constraint is reached and therefore the water injection decreases (Fig. 19) for both the BC and the BC-GCC. The decrease in the water injection results in less water production and hence water cut. Due to the lower water produc-

tion oil production is increased, without a better sweep efficiency being proved.

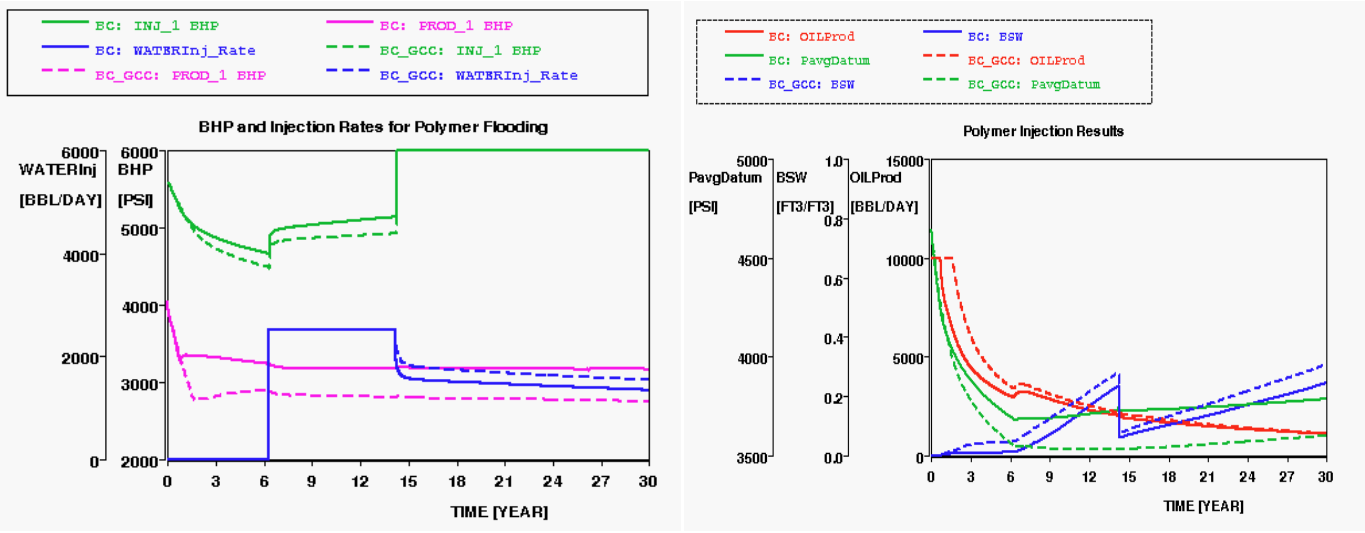

Fig. 19: (a) BHP for the producer and the injector in BC and BC-GCC, (b) Oil production, water cut and average datum pressure profiles for BC and BC-GCC during polymer flooding.

To investigate if a better sweep efficiency is obtained by using polymer the BHP constraint was increased so that 2500bbl/day of water can be injected constantly. This increase resulted in an increase in water cut as more water is being produced, but also in an increase in oil production indicating that better sweep efficiency is achieved. The final recovery factor was increased 0.5% more. The overall increase in the recovery factor with the polymer flooding is 1%, but this value corresponds to the higher BHP constrain case, which in reality could be applied by adding a second well in the sector model. The increase in recovery with the polymer is low compared to water injection and as polymer is more expensive the economic viability of this method must be further investigated before applying it.

Sweep efficiency comparison. A comparison of the sweep efficiency for the water injection, the WAG and the polymer flooding is presented in Fig. 20. The location of the producer is at -8800ft. From -8800ft till -7061.9ft the sweep efficiency of the gas injection at the gas cap is illustrated, which is the same for water injection and the polymer case, but slightly lower for the WAG case, as due to the gas constraint less gas is being injected from the gas cap during WAG. Important information is presented in the section from -10000ft till -8800ft, which illustrates the sweep efficiency for water injection, WAG and polymer flooding respectively. For the WAG, higher sweep than water injection and polymer flooding is observed after 30 years, with 0.1-0.2 increase (Fig. 21). The increase in oil production with WAG is therefore based on the better sweep efficiency (Appendix K). The difference in sweep between water injection and polymer is small, with polymer having slightly higher sweep.

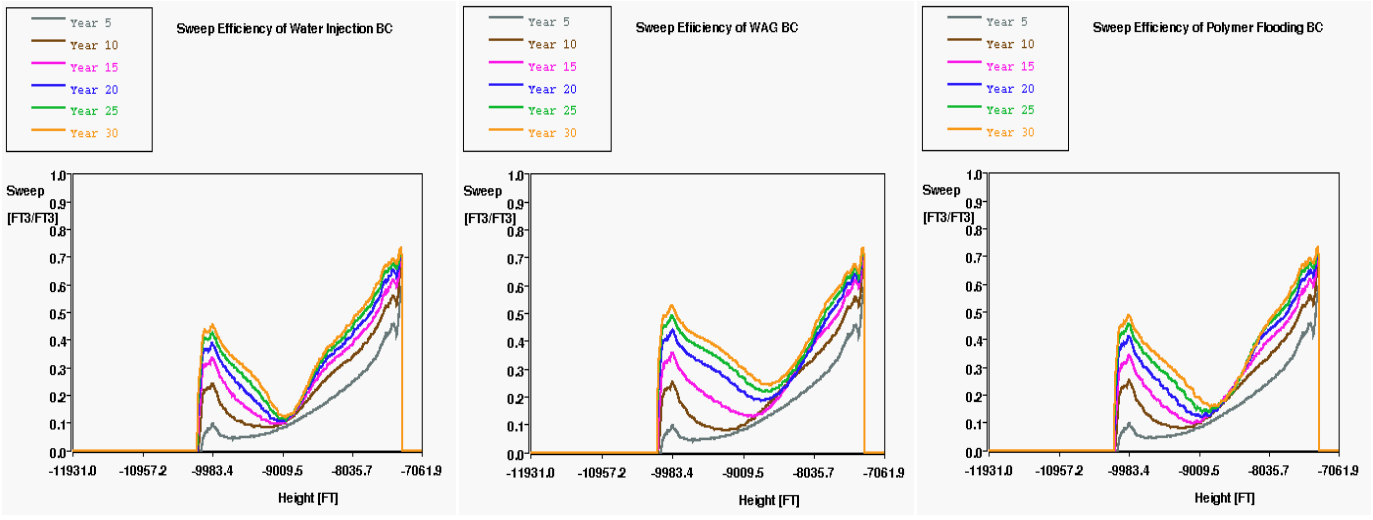

Fig. 20: Sweep efficiency for (a) water injection, (b) WAG and (c) polymer flooding for different years.

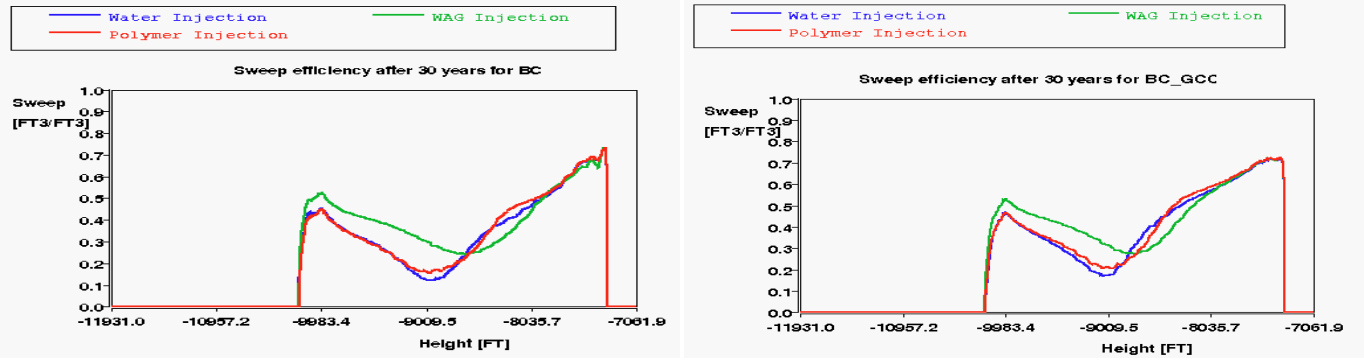

Fig. 21: Sweep efficiency comparison of water injection, WAG and polymer flooding after 30 years for BC and BC_GCC.

Discussion

An investigation of the water injection performance in Pierce was completed in this study using theoretical analysis methods, data integration and reservoir simulation tools. Based on the Buckley-Leverett and the Dykstra-Parson methods, layering was proved to have the highest impact on breakthrough time regarding sweep efficiency, due to the turbidite nature of the field. The DP method can provide a good estimation of the breakthrough time in turbidite fields and should be used to understand water displacement mechanisms prior toreservoir simulation. The results from the DP are only estinations as the method assumes total continuity of the layers, however in a turbidite field layering discontinuities are present. Data integration gave significant information regarding communication between wells, water flow and pressure support. Although, uncertainty regarding the quality of the data resulted in difficulties on analyzing and combining them. Two cases have been identified across the field, one with early gas breakthrough and one with late gas breakthrough and aquifer support.

Reservoir simulation was used for simulating and predicting flow behaviour for water injection, WAG and polymer flooding using a sector model. The sector model was populated according to the field properties, but it is not an exact sector from the static model and hence there is high uncertainty around certain parameters. The water cut and the recovery are highly sensitive to permeability and permeability anisotropy ratio and less to the Corey parameters and grid block size. Others parameters that affect the results but have not been investigated are the model dimensions, fracturing of the reservoir, variation in horizontal permeability, the sequence of the layers and the tilting of the OWC. By increasing the model dimensions, the distance between the producer and the injector increases as well, giving water the ability to flow towards all directions and not only straight towards the producer. A single constant value of horizontal permeability across each layer results in water moving faster horizontally. However, the turbidite reservoir consists of shale layers of different length, so varied permeabilites across the same layer would result in water flowing through more complicated paths. The formation of the salt diapirs and their movement upwards results in the compression of some layers, but there is uncertainty on whether these are the top or the bottom layers of the structure. This compression affects the sequence of the layering, resulting in variation in flow. In various sections of the field different OWC have been observed indicating tilting of the OWC, but in this study this tilting has not been modelled.

Past studies in Pierce (Hustedt and Snippe) tried to explain the behaviour of water injection based on fracturing. However, from this study the early breakthrough can be attributed to the high permeability layers. Water injection proved to be insensitive to the type and the location of the injector as the high permeability layers and the k_v/k_h ratio have the highest impact on flow behaviour, with only the perforation strategy making a difference in the overall recovery. Higher injection rates have a small impact in oil production, as due to high water cut the water ends up circulating in the field and not actually increasing sweep. WAG injection increased the sweep efficiency and the ultimate recovery and it is considered as possibly economically viable, as gas is already being produced and injected. Polymer flooding for a low injector BHP constraint provides the same recovery as simple water injection, but for an increase in BHP, which in reality would mean using a second injector from the ones already existing or adding a new one as the injectors in the field have a significant distance between them, higher recovery is observed. However, as this recovery is lower than the one obtained from WAG and the cost for the polymer and an additional injector is high, the economical viability of this method is not certain. As polymer injection has been modelled with an increase in water viscosity and not as a fourth phase there is high uncertainty on the results. In order to reduce the uncertainty modelling a fourth phase would be necessary.

Conclusions and Recommendations

The following conclusions may be drawn based on this study:

- For analytical estimations of water breakthrough time in turbidite reservoirs, the Dykstra-Parsons method should be used.
- Flow behaviour is dominated by the highly permeable layers.
- Permeability and permeability anisotropy ratio have the highest impact to water cut and cumulative oil production.
- Higher injection rates do not increase sweep efficiency, as water is being circulated in the field, so a low water injection

strategy is more beneficial.

- In turbidite reservoirs with high variation in permeability, a selective perforation strategy can increase oil production by perforating only the low permeability layers. The type and the location of the injector do not affect oil production.
- WAG injection proved to be successful, as residual oil saturation decreases. The increase in the recovery factor was estimated at 2-2.5%.
- Polymer flooding proved to be less successful than WAG regarding sweep efficiency, but high uncertainty governs the results, due the way it was modelled.

For this study, a sector model approach has been used, however the findings should be also verified using the dynamic model of the field, once it is completed. The variation in horizontal permeability, the sequence of the layers and the tilting of the OWC should be investigated as these parameters have not been considered in this paper. Polymer efficiency should be investigated by adding a fourth phase.

Nomenclature

BC	Base Case	μ_w	Viscosity of water (cP)
BC-GCC	Base Case-Gas Cap Constrained	NTG	Net to gross
BHP	Bottomhole pressure (psi)	N_w	Corey exponent for water relative permeability
d_{inj}	Distance between injection wells (ft)	N_o	Corey exponent for oil relative permeability
$d_{inj,prod}$	Distance between injectors and producers (ft)	OWC	Oil water contact
f_w	Fractional flow of water	q_i	Water injection rate (bbl/day)
GOC	Gas oil contact	S_w	Water saturation
h_i	Layer thickness (ft)	$S_{w,bt}$	Water saturation at breakthrough
h_{res}	Reservoir thickness (ft)	S_{wc}	Connate water saturation
k_{ro}	Relative permeability to oil (mD)	S_{or}	Residual oil saturation
k_{rw}	Relative permeability to water (mD)	W_{id}	Dimensionless cumulative water injected
k_v/k_h	Permeability anisotropy ratio	ϕ	Porosity
M	Mobility ratio (pore volumes)		
μ_o	Viscosity of oil (cP)		

Acknowledgements

The author is grateful to Shell U.K. Limited for their support during this academic year.

References

Buckley, S.E and Leverett, M.C. *et al*.: "Mechanism of Fluid Displacement in Sands", Trans. AIME (1942), 146, 107-116.

Dake, L.P.: *Fundamentals of Reservoir Engineering*, first edition, Elsevier, Amsterdam, (1978), 344-372.

Dake, L.P.: *The Practice of Reservoir Engineering*, revised edition, Elsevier, Amsterdam, (1994), 413-425.

Dennis, H., Baillie, J., Holt, T. and Wessel-Berg, D. *et al*.: "Hydrodynamic Activity and Tilted Oil-Water Contacts in the North Sea", Norwegian Petroleum Society Special Publications (2000), 9, 171-185.

Dykstra, H. and Parsons, R.L.: "The Prediction of Oil Recovery by Water flood", Secondary Recovery of Oil in U.S., API (1950), 160.

Farouq A. S.M. and Thomas S. *et al*.: "The Promise and Problems of Enhanced Oil Recovery Methods", paper SPE SS-89-26 presented at the 1989 Technical Meeting/Petroleum Conference of The South Saskatchewan Section, Regina, Sept. 25-27.

Hustedt, B. and Snippe, J.R. *et al*.: "Integrated Data Analysis and Dynamic Fracture Modelling Key to Understanding Complex Water floods: Case Study of the Pierce Field, North Sea", *SPEREE* (Feb. 2010), 13.

Kyte, J.R., Stanclift, Jr. R.J. and Rapoport, L.A. *et al*.: "Mechanism of Water Flooding in the Presence of Free Gas", Trans. AIME (1956), 207, 215-221.

Lake, L.W.: Enhanced Oil Recovery, first edition, Prentice Hall Professional, (1996), (314-353).

Van Daalen, F. and Van Domselaar, H.R. *et al*.: "Water Drive in Inhomogeneous Reservoirs – Permeability Variations Perpendicular to the Layer", *SPEJ* (Jun. 1972), 12 (3), 211-219.

Van Nispen, D.J., Hunt, J., Hartwijk, A. and Trofimov, A. *et al*.: "Application of Smart, Fractured Water Injection Technology in the Piltun-Astokhskoye Field, Sakhalin Island, Offshore Russia", paper SPE 102310 presented at the 2006 SPE Russian Oil and Gas Technical Conference and Exhibition, Moscow, Russia, Oct. 3-6.

Welge, H.J. *et al*.: "A Simplified Method for Computing Oil Recovery by Gas or Water Drive", Trans. AIME (1952), 195, 91-98.

Wu, X., Ogbe, D.O., Zhu, T. and Khataniar, S. *et al*.: "Critical Design Factors and Evaluation of Recovery Performance of Miscible Displacement and WAG Process", paper SPE 2004-192 presented at the 2004 Canadian International Petroleum Conference, Calgary, Alberta, Jun. 8-10.

Appendix A: Literature Review

SPE Paper N^o	Year	Title	Authors	Contribution
942107-G	1942	Mechanisms of Fluid Displacement in Sands	S.E. Buckley, M.C. Leverett	First to describe the mechanism of fluid displacement from water and gas in homogeneous reservoirs.
-	1950	The Prediction of Oil Recovery by Water flood	H. Dykstra, R.L. Parsons	First to describe the mechanism of fluid displacement in stratified reservoirs.
124-G	1952	A Simplified Method for Computing Oil Recovery by Gas or Water Drive	H. J. Welge	A simplified method for computing oil recovery without using numerical integration was proposed.
536-G	1956	Mechanism of Water Flooding in the Presence of Free Gas	J.R. Kyte, R.J. Stanclift Jr., S.C. Stephan Jr., and L.A. Rapoport	Provided an explanation about the mechanism and the effect of the presence of free gas in water flooding.
3358-PA	1972	Water Drive in Inhomogeneous Reservoirs - Permeability Variations Perpendicular to the Layer	F. Van Daalen, H.R. Van Domselaar	Studied the effect of permeability variations in oil recovery.
SS-89-26	1989	The Promise and Problems of Enhanced Oil Recovery Methods	S.M. Farouq Ali, S. Thomas	Examines the applicability of EOR methods in the field, in terms of mobility ratio and capillary number.
102310-MS	2006	Application of Smart, Fractured Water Injection Technology in the Piltun-Astokhskoye Field, Sakhalin Island, Offshore Russia	D.J. van Nispen, J.Hunt, A. Hartwijk, A. Trofimov	Describes the application of fractured water flood using field examples.
132440-PA	2010	Integrated Data Analysis and Dynamic Fracture Modelling Key To Understanding Complex Water floods: Case Study of the Pierce Field, North Sea	B. Hustedt, J.R. Snippe	The role of fracturing in Pierce water flooding.

SPE 942107-G (1942)

Mechanism of Fluid Displacement in Sands

Authors: Buckley S. E. and Leverett M. C.

Contribution to the understanding of fluid displacement:
High, as it was the first to describe the displacement of oil by water or gas.

Objective of the paper:
To describe the mechanism by which oil is displaced by water or gas in sands and the conditions affecting it.

Methodology used:
A theoretical approach was used, in order to investigate the displacement of oil by gas or water. A material balance equation was used and transformed to

$$\left(\frac{\partial u}{\partial \theta}\right)_{S_D} = -\frac{q\tau}{qA}\left(\frac{\partial f_D}{\partial S_D}\right)_{\theta} \qquad \text{(Eq. A-1)}$$

and f_w vs. S_w and S_w vs. distance, u, were plotted to calculate saturation history during water flood.

Conclusion reached:

1. From (Eq.A-1) it is implied that the rate of advance of a plane that has a certain fixed saturation is proportional to the change in composition of the flowing stream caused by a small change in the saturation of the displacing fluid.
2. The displacing fluid moves from a region of high saturation into one of lower saturation and removes oil, converting the invaded region to one of higher saturation in the displacing fluid. In all cases, both the oil and the displacing fluid flow together and simultaneously through the same pores. The method proposed calculates the saturation distribution behind the front, the interface between the displaced and the displacing phases.
3. During displacement, the permeability of the sand to oil will continuously decrease and that of the displacing fluid will increase (initial phase of displacement), until large volumes of displacing fluid will result in removal of only a slight amount of additional oil (subordinate phase of the displacement).
4. Conditions affecting displacement:
    - Viscosity: The more viscous the oil, the less readily it flows under a given pressure gradient. Increased oil viscosity therefore results in the attainment of lower water saturation during the initial phase of the displacement as well as more gradual approach to the residual oil saturation during the subordinate phase of the displacement.
    - Initial fluid saturation: If before invasion by the displacing fluid the saturation of the displacing fluid in the sand exceeds that which would be obtained during the initial phase of the displacement, this phase will be absent abd only the subordinate phase will occur. This could be encountered in a water drive operation in tight sands, with viscous oils, or in thin oil sands immediately overlying water.
    - Capillary and Gravitational forces: Capillary forces tend to oppose the formation of saturation discontinuities in a homogeneous sand, while gravitational forces tend to promote complete vertical segregation of oil, gas and water.

Comments:
The equation derived from Buckley – Leverett describes immiscible displacement in one dimension for sands.

SPE 124-G (1952)

A Simplified Method for Computing Oil Recovery by Gas or Water Drive

Authors: Welge H.J

Contribution to the understanding of fluid displacement:
It provides a simplified analytical method for computing the oil recovery.

Objective of the paper:
To provide a simplified analytical method for calculating oil recovery without using numerical integrations and requiring knowledge of relative permeability for a limited saturation range.

Methodology used:
Used the methodology proposed by Buckley and Leverett (1942) and derived a simplified method for calculation of oil recovery by using the equation $S_{av} - S_2 = (f_{oil})_2 \, Q_1$ for a gas drive, where S_{av} is the total fractional recovery of oil. An illustrative example of the Mile Six Pool in Peru has been used to confirm the proposed method of calculation.

Conclusion reached:
1. The maximum slope of the tangent, which corresponds to the highest velocity the gas saturation moves can be used in conjunction with $\left(\frac{\Delta x}{\Delta t}\right)_S = uf'$ to obtain the time of gas breakthrough at the producing wells.
2. For fields that have been exploited by dissolved gas drive for a time before gas injection, this method can be used, except that at the end of the computations the time scale must be aligned in relation to calendar time.
3. The method described for a gas drive can be applied equally well for water flooding.
4. The relations derived can also be used for the calculation of relative permeability ratio from laboratory displacement data.

Comments:
In this paper the displacement fluid is assumed to be incompressible and immiscible with the oil and flow is in one dimension.

SPE 536-G (1956)

Mechanism of Water Flooding in the Presence of Free Gas

Authors: Kyte J.R., Stanclift Jr. R.J., Stephan Jr. S.C., and Rapoport L.A.

Contribution to the understanding of fluid displacement:
High, as it explains the mechanism and the effect of the presence of free gas in water flooding.

Objective of the paper:
To determine the type of displacement mechanism occurring when water invades a porous medium containing oil and a mobile gas phase. To investigate the effect of free gas on water flood oil recovery for a wide range of core materials and fluid properties.

Methodology used:
An experimental procedure was followed and seven cores representing five different types of water-wet and oil-wet porous media were used in order to conduct 44 flooding tests. Three types of operations were carried out: one reference water flood performed without any free gas in the core, to provide a standard of comparison (14 tests), one water flood in presence of a mobile gas phase (14 tests) and one water flood in presence of a trapped gas phase (16 tests).

Conclusion reached:
1. The injection of water in a medium containing oil and free gas results in the formation of an oil bank which displaces part of the initial free gas phase, but leaves behind a certain residual, trapped gas saturation.
2. The residual oil saturations by water flooding in the presence of gas are lower than those obtained in the absence of gas and a higher oil recovery is achieved.
3. For a given porous medium and fluid system there is a unique relationship between (a) the trapped gas saturation and the initial mobile gas saturation, (b) the oil saturation attainable at any one flooding stage and the trapped gas saturation existing in the porous medium during the flood, and (c) the oil saturation attainable at any one flooding stage and the initial mobile gas saturation.
4. The use of simplified procedures for flooding test on short core samples to evaluate the reduction in residual oil caused by the presence of a gas phase has been justified.

Comments:
The results obtained from the experimental studies are representative of the situation where the effects of gas compressibility and solubility are negligible.

SPE 3358-PA (1972)

Water Drive in Inhomogeneous Reservoirs - Permeability Variations Perpendicular to the Layer

Authors: Van Daalen F., Van Domselaar H.R.

Contribution to the understanding of fluid displacement:
High, as it explains the displacement mechanism in inhomogeneous reservoirs with permeability variations perpendicular to the layer.

Objective of the paper:
Equations were derived for a two-dimensional water drive in a porous system with either continuously or a discontinuously varying permeability distribution perpendicular to the layer.

Methodology used:
Used the theories developed by Beckers H.L (1965) and Dietz D.N. (1953) in order to arrive at an analytical expression for the oil production from an inhomogeneous system.

Conclusion reached:

1. It is incorrect to use an average permeability for the calculations as the oil production curves varied according to the permeability.
2. When the permeability increases continuously in an upward direction recovery is higher than in the homogeneous case and when the permeability decreases upwards, a lower recovery is obtained.
3. A fracture-type permeability distribution, clearly demonstrates the favorable effect of a zone of high permeability at the top of the producing layer. A fracture at the bottom would have an adverse effect on the vertical sweep efficiency.

Comments:
The influence of capillary forces has not been taken into account. A necessary condition for the validity of the equations is that the water should underrun the oil, the layer has uniform thickness and the flow is two-dimensional.

SPE SS-89-26 (1989)

The Promise and Problems of Enhanced Oil Recovery Methods

Authors: Farouq A. S.M., Thomas S.

Contribution to the understanding of fluid displacement:
Low, as it analyses the promises and problems of the EOR methods according to research by others.

Objective of the paper:
To outline in a systematic and balanced manner the impact of the EOR methods according to field experience.

Methodology used:
Each method is described according to the effect it has on improving the mobility ratio and increasing the capillary number. The methods discussed are polymer flooding, miscible displacement, carbon dioxide flooding, microemulsion flooding, steam injection and in situ combustion.

Conclusion reached:

1. Many EOR methods look good in the laboratory but fail in the field, due to the inability of carrying out scaled experiments.
2. Steam injection was proved to have a high chance of success, miscible displacement may be successful under special conditions and carbon dioxide flooding may have potential but needs further investigation.
3. Microemulsion flooding was proved successful in the field, but was considered complex and costly.
4. Polymer flooding may yield modest incremental oil. Alkaline and surfactant floods are of great research potential, but high risk field processes.
5. Research must continue on EOR methods as well as field testing.

Comments:
In this paper the EOR methods are discussed from a mechanistic point of view, explaining the technical limitations and the differences in their performance from the laboratory to the field.

SPE 102310-MS (2006)

Application of Smart, Fractured Water Injection Technology in the Piltun-Astokhskoye Field, Sakhalin Island, Offshore Russia

Authors: Van Nispen D.J, Hunt J., Hartwijk A., Trofimov A.

Contribution to the understanding of fluid displacement::
It describes fractured water flooding.

Objective of the paper:
To describe the application of fractured water flood using field examples.

Methodology used:
Water injection above the fracture pressure was tested with a fracture simulation tool for the Piltun and Astokh area. Initially, sea-water is used, which gradually is replaced by produced water.

Conclusion reached:

1. Permanent downhole gauge data are critical for improving reservoir understanding and monitoring fracture growth.
2. Fractured water injection in Astokh has delivered injection performance equal to or better than could be expected from matrix injection with zero skin.
3. Analysis of fall-off data indicates that the induced fractures are smaller than expected
4. Based on Astokh experience, Piltun injection wells have been designed with low inclination through the reservoir to reduce tortuosity effects and maximize injectivity.
5. In multi-layer reservoirs, selectivity is required to ensure fractures are initiated and water is injected into all layers.

Comments:
Suggestions from this paper have been used in this study.

SPE 132440-PA (2010)

Integrated Data Analysis and Dynamic Fracture Modelling Key to Understanding Complex Water floods: Case Study of the Pierce Field, North Sea

Authors: Hustedt B., Snippe J.R.

Contribution to the understanding of fluid displacement:
High, as it uses dynamic fracture modelling to understand water flooding of Pierce Field.

Objective of the paper:
To investigate the performance of water flooding characterized by fluid injection under fracturing conditions in the Pierce Field, North Sea.

Methodology used:
Analysis of raw data (daily injection/production rates and THP/BHP), stress data and well-test interpretation. For the fracture modelling, FRAC-IT simulator was used to study the dynamic fracture propagation.

Conclusion reached:

1. A vertically contained fracture was indicated from the results with half-length of 700-850 ft and height of 50-100 ft.
2. Dynamic fractures on the order of the well spacing under historical injection rates are a major concern for any water-injection strategy in Pierce.
3. Maximum injection rates must be set for injectors in order to keep expected fracture sizes well below the well distance and to give better areal sweep.

Comments:
The main improvement compared to previous work was the integration of data analysis and the dynamic modelling work, rather than looking at each data source individually.

Appendix B: Pierce Field

Objective: This section presents maps of the Pierce field.

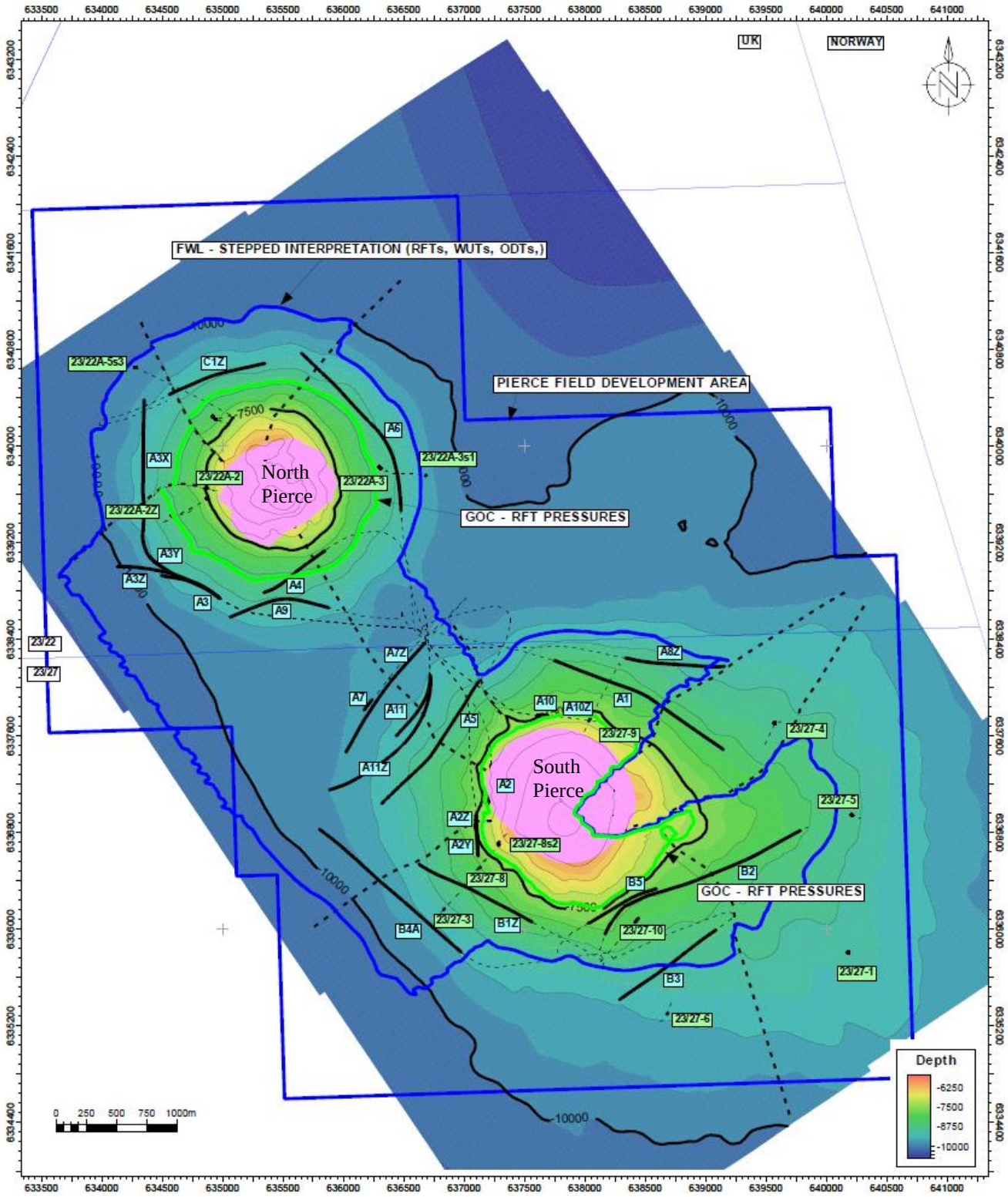

Fig.B- 1: Depth map of North and South Pierce, presenting all wells.

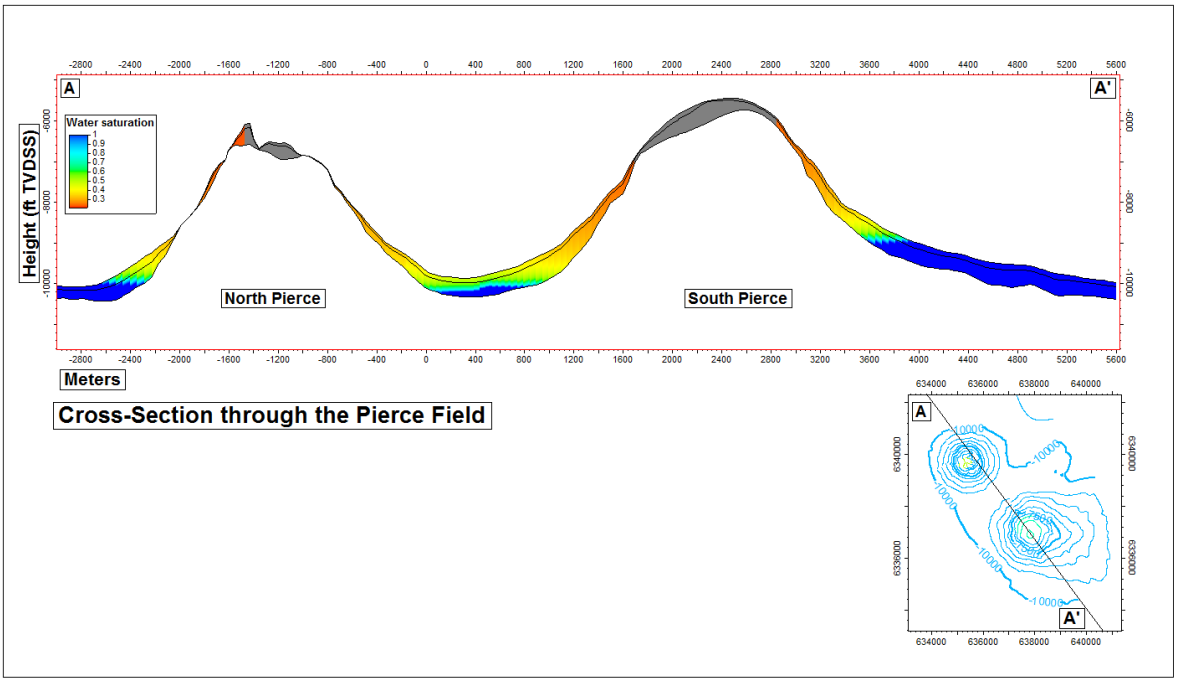

Fig.B- 2: Cross section of saturation through Pierce.

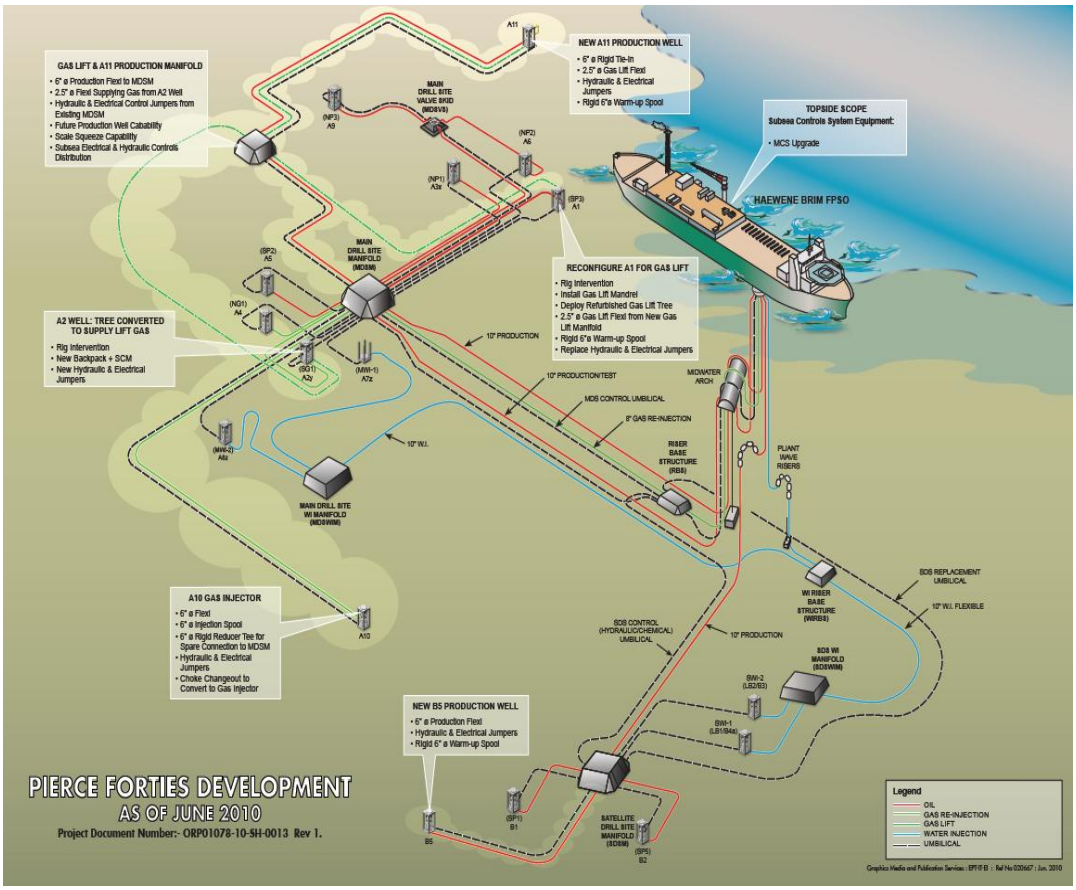

Fig.B- 3: Pierce subsea facilitites.

Appendix C: Buckley-Leverett Analysis

Objective: This section presents the Buckley Leverett method as proposed by Dake (1978).

The Buckley-Leverett method describes immiscible displacement in one dimension in homogeneous reservoirs and provides the basic equation for oil displacement by water, which is

$$\left.\frac{dx}{dt}\right|_{S_w} = \frac{q_t}{A\phi}\left.\frac{df_w}{dS_w}\right|_{t} \tag{C-1}$$

where the fractional flow equation of water is

$$f_w = \frac{q_w}{q_t} = \frac{q_w}{q_w+q_o} = \frac{1-\frac{kk_{ro}A}{q_t\mu_o}\frac{\Delta\rho\, g\sin\theta}{1.0133x10^6}}{1+\frac{\mu_w\, k_{ro}}{k_{rw}\,\mu_o}} \tag{C-2}$$

And if the capillary gradient is neglected and gravity segregation is negligible Eq. A-2 can be reduced to

$$f_w = \frac{1}{1+\frac{\mu_w\, k_{ro}}{k_{rw}\,\mu_o}} \tag{C-3}$$

The shock front saturation occurs at the tangent to the water fractional flow (Welge 1952) and can be determined graphically by plotting the water fractional flow vs saturation (Fig.C- 1).

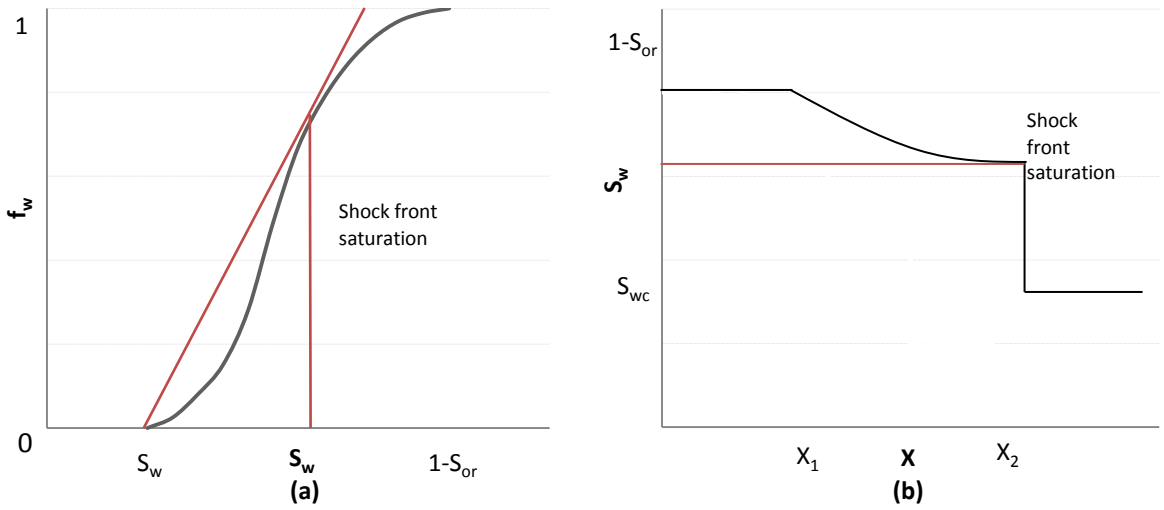

Fig.C- 1: (a) Typical water fractional flow curve as a function of saturation presenting shock front saturation, (b) Water saturation distribution as a function of distance at breakthrough.

Appendix D: Dykstra-Parsons Method

Objective: This section presents the Dykstra-Parson method as proposed by Dake (1994).

The Dykstra-Parsons method describes the displacement of fluids in stratified reservoirs. This method can calculate vertical sweep efficiency for all values of the mobility ratio and caters for velocity dispersion of the flood front between the individual layers. For the mobility ratio (Fig.D- 1), if:

- M < 1: the velocity of frontal advance in each layer will be reduced as the flood progresses, which tends to stabilize the macroscopic flood front.
- M > 1: the velocity of frontal advance in each layer increases as the flood progresses which promotes instability in the macroscopic flood front.

According to this method, Darcy's law can be applied at the flood front during the flooding of an individual layer in which it is assumed that piston-like displacement occurs. The position of the front is given by

$$\frac{1}{2}Ax_j^2 + x_j = \frac{\lambda_j}{\lambda_i}\left(\frac{1}{2}A + 1\right) \tag{D-1}$$

where,

$$\lambda = \frac{kk'_{rw}}{\phi \Delta S_w} \tag{D-2}$$

$$A = \frac{1}{M} - 1 \tag{D-3}$$

The expression in Eq. D-1 is valid for all layers and calculates the position of the front in the *j*th layer, still to flood, when the *i*th layer of the section has been flooded with water. As each layer floods, the frontal positions in all the remaining unflooded layers can be calculated by solution of the quadratic Eq. B-2. The order in which the layers flood can be predicted in decreasing sequence of λ. The fractional flow for a section of fixed width, w, and individual layer thickness, h_i, can be calculated by

$$f_w = \frac{\sum_{i=1}^{n} \frac{\lambda_i h_i}{A+1}}{\sum_{i=1}^{N} \frac{\lambda_i h_i}{Ax_i+1}} \tag{D-4}$$

The numerator represents flow in the flooded layers and the denominator across the total section.

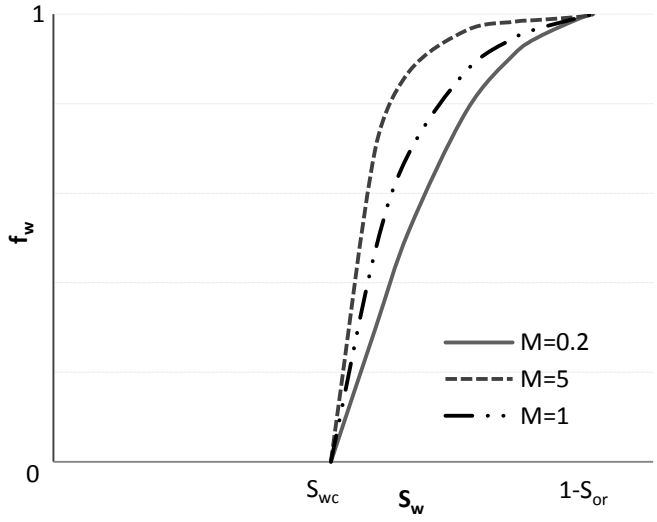

Fig.D- 1: Dykstra-Parsons fractional flow curves for different mobility ratios.

Appendix E: South Pierce Data

Objective: This section presents production and injection data for the entire South Pierce and not for each well separately.

In Fig.E- 1 production data are presented for South Pierce. From the pressure data with the start of production pressure depletion is observed. After water injection starts two pressure profiles are observed one that respond quickly to the water injection and hence pressure increases and one with delayed pressure response.

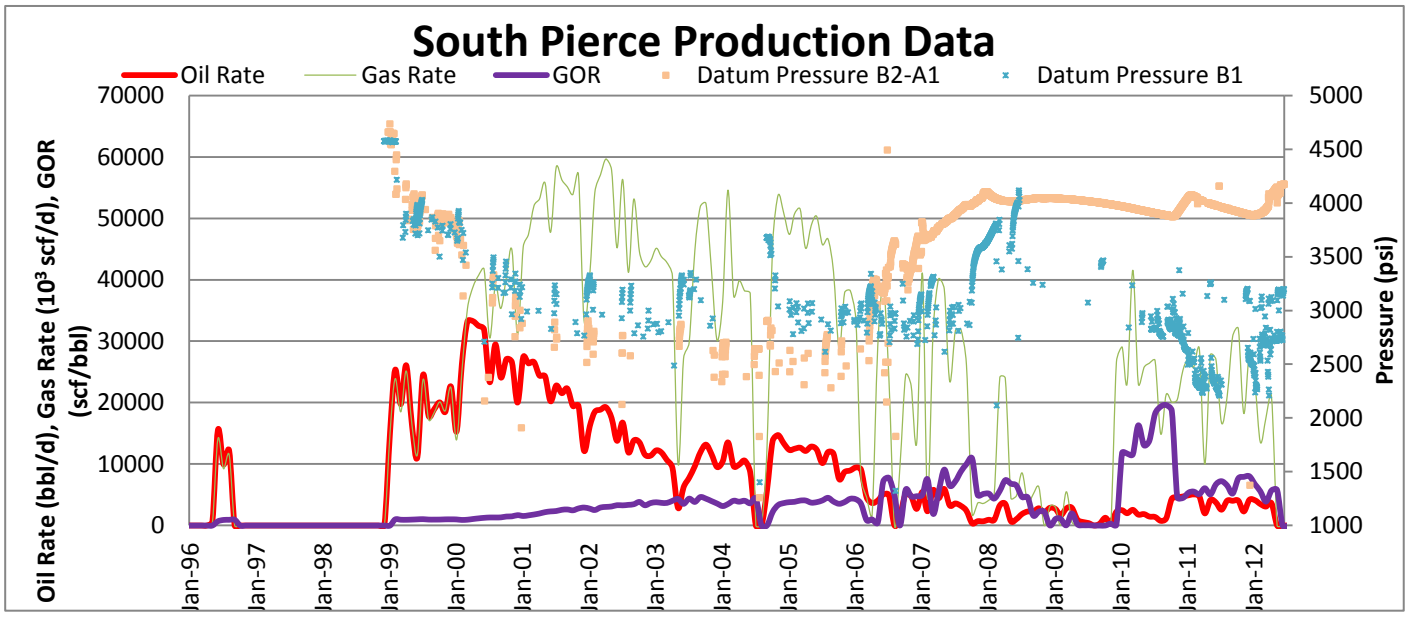

Fig.E- 1: Cumulative oil rate, cumulative gas rate, GOR and datum pressures for South Pierce.

In Fig.E- 2 presents the injection data for South Pierce. After water injection high increase in water cutis observed.

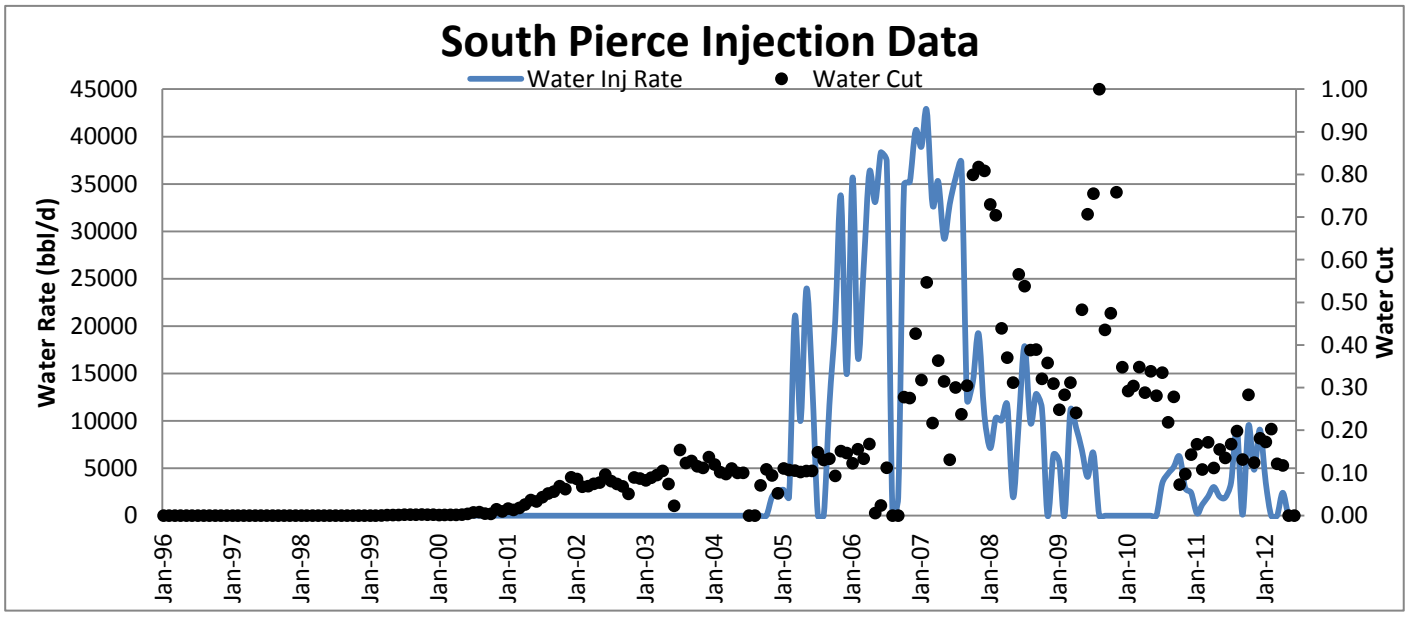

Fig.E- 2: Cumulative water injection rate and water cut for South Pierce.

Appendix F: Water Tracer Experiments

Objective: This section explains the water tracer measurements and provides the relevant data.

Water tracer measurements: A technique in which a tracer (a chemical or isotopic marker) is injected into the flow stream of an injection well to determine fluid paths and communication with a production well. Communication between the wells is indicated if the tracer is found in samples collected from the producer.
The map (Fig.F- 1) presents the water tracer strategy that was followed and the results from the sample analysis are presented in

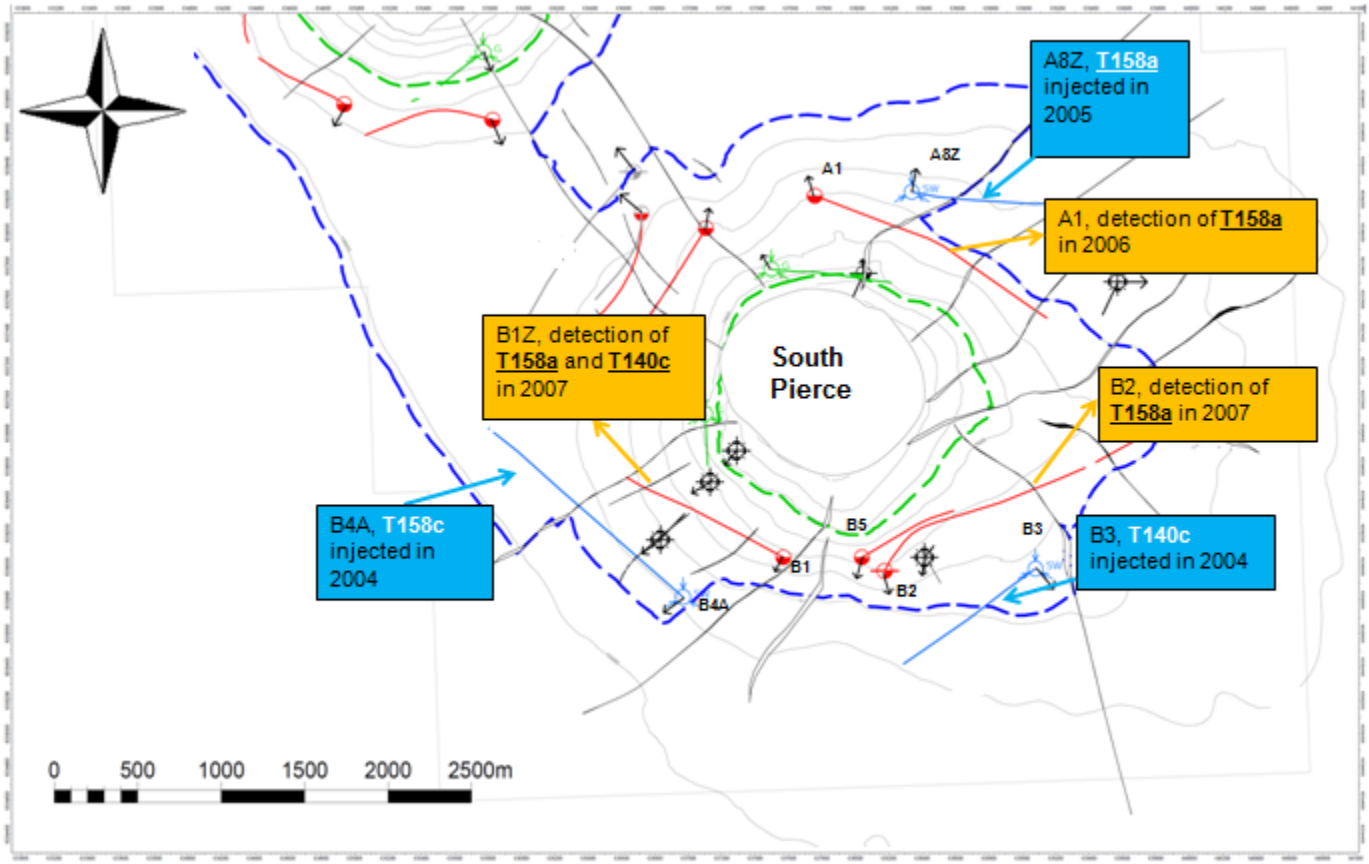

Fig.F- 1: Water tracer experiments map.

Sample Analysis: 08.06.06 (JS 15773)			
Reference	Well reference	Sample Details	158a ppb w/w
42915	Sat Flowline B2+B1Z	24.05.06 – 08:00	ND
42916	Sat Flowline B2+B1Z	24.05.06 – 19:30	ND
42917	Flowline 2 Well A1	27.05.06 – 09:00	228±23
42918	Flowline 2 Well A1	27.05.06 – 14:30	229±23
42919	Flowline 2 Well A1	28.05.06 – 04:00	234±23
42920	Flowline 2 Well A1	28.05.06 – 09:00	234±23
42935	Haewene Brim Well A1 Test Sep	12.05.06 – 07:15	163±16
42936	Haewene Brim Well A1 Test Sep	12.05.06 – 08:30	157±16

Samples Analysis: 30.03.07 (JSJM 16913)						
Reference	Well Reference	Sample Details	T-140c ppb w/w	T-158a ppb w/w	T-140a ppb w/w	T-158c ppb w/w
52945	B2	19.03.07	ND	ND	ND	ND

Samples Analysis 15.05.07 (KB 17092)						
Reference	Well Reference	Sample Details	T-140c ppb w/w	T-158a ppb w/w	T-140a ppb w/w	T-158c ppb w/w
54605	B2	07.05.07	ND	ND	ND	ND

Samples Analysis 06.06.07-11.06.07 (JSMH 17913)						
Reference	Well Reference	Sample Details	T-140c ppb w/w	T-158a ppb w/w	T-140a ppb w/w	T-158c ppb w/w
55565	B1Z+B2	2007-02894 28.05.07 11:30	ND	12±1.2	ND	ND
55712	B1Z±B2	2007-2965 8:45	ND	8.0±0.8	ND	ND

Sample Analysis 23.07.07-25.07.07 (DB 17354)						
Reference	Well Reference	Sample Details	T-140c ppb w/w	T-158a ppb w/w	T-140a ppb w/w	T-158c ppb w/w
57089	B1Z	2007-03726 11.07.07	ND	18±2	ND	ND
57110	B1Z	2007-03835 15.07.07	ND	6.3±0.6	ND	ND

Samples Analysis: 25.07.07 (JS LF 17252)						
Reference	Well Reference	Sample Details	T-140c ppb w/w	T-158a ppb w/w	T-140a ppb w/w	T-158c ppb w/w
55973	B1Z & B2	18.06.07	ND	8.7±0.9	ND	ND

Samples Analysis 31.07.07 (JS 17411)						
Reference	Well Reference	Sample Details	T-140c ppb w/w	T-158a ppb w/w	T-140a ppb w/w	T-158c ppb w/w
57201	B1Z	2007-03933 25.07.07	ND	11±1.1	ND	ND

Samples Analysis 02.10.07 (JSAP 17648)						
Reference	Well Reference	Sample Details	T-140c ppb w/w	T-158a ppb w/w	T-140a ppb w/w	T-158c ppb w/w
59487	B1Z	2007-04968 22.09.07 09:45	ND	ND	ND	ND
59588	B1Z	2007-05030 26.09.07 08:30	6.0±0.6	ND	ND	ND
59591	B1Z Sat Flow	2007-05030 01.10.07 14:00	6.5±0.7	ND	ND	ND

Table F. 1: Tracer sample analysis data.

Appendix G: Sector Model Flow Chart

Objective: This section presents the sector model flow chart.

Fig.G- 1 presents the construction of the sector model. Initially, the dimensions, the size of the gridblocks, the dip and the phases of the model were selected. Once the sector was created, the geological, relative permeability and PVT data were inputed. Three wells were constructed and the model was initiallised. Once the simulation runs, results are obtained.

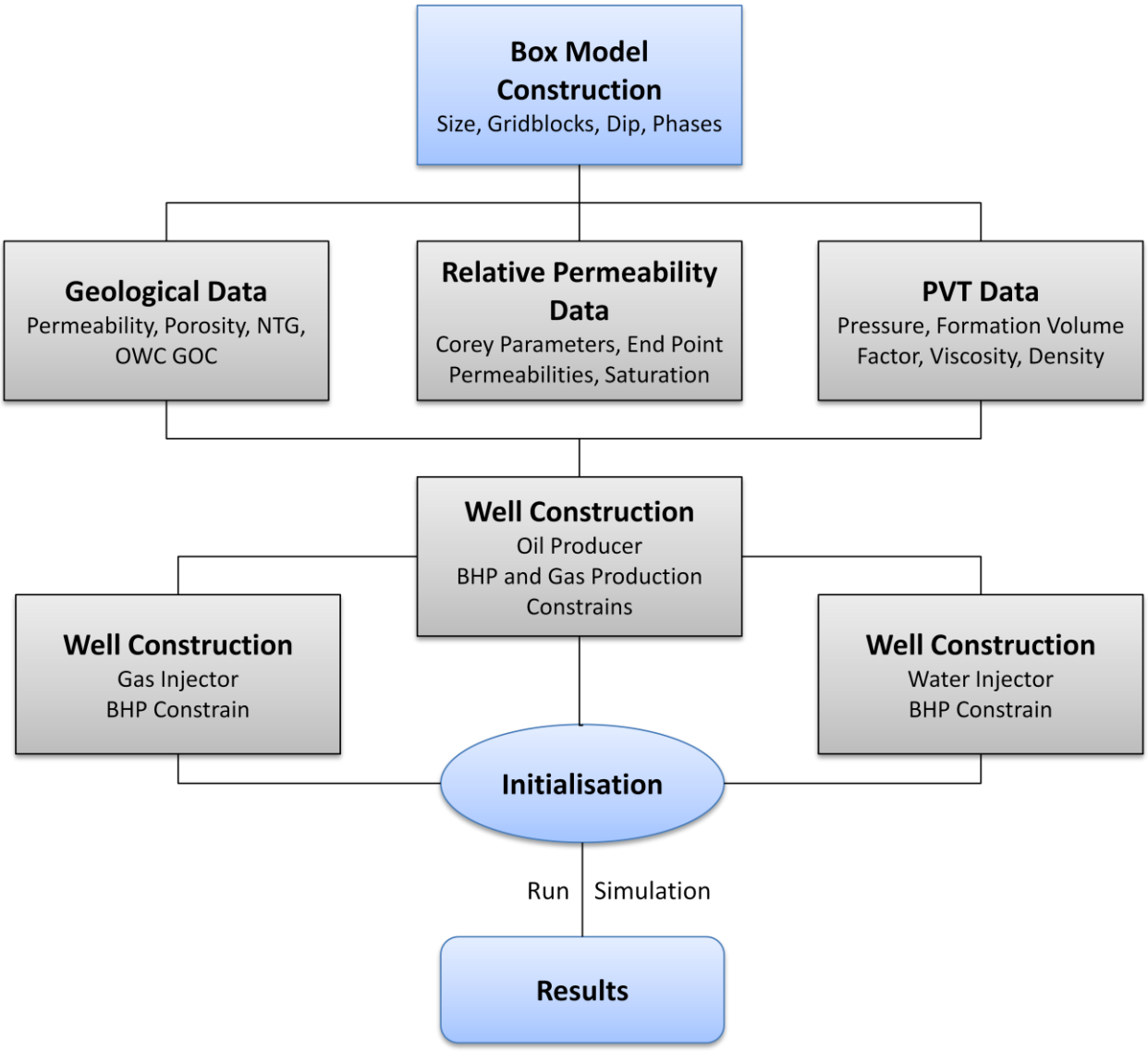

Fig.G- 1: Flow chart presenting the way the sector model was constructed.

Appendix H: Simulation Results for Base Case (BC) and Base Case-GCC (BC-GCC)

Objective: This section presents the simulation results for the BC and the BC-GCC.

Fig.H- 1and Fig.H- 2 illustrate the saturation profiles for a low and high permeability layer for the BC. In the low permeability profiles gas moves slowly towards the producer, while water mobility is only observed after 10 years. In contrast, in the high permeability profiles both phases move quickly towards the producer.

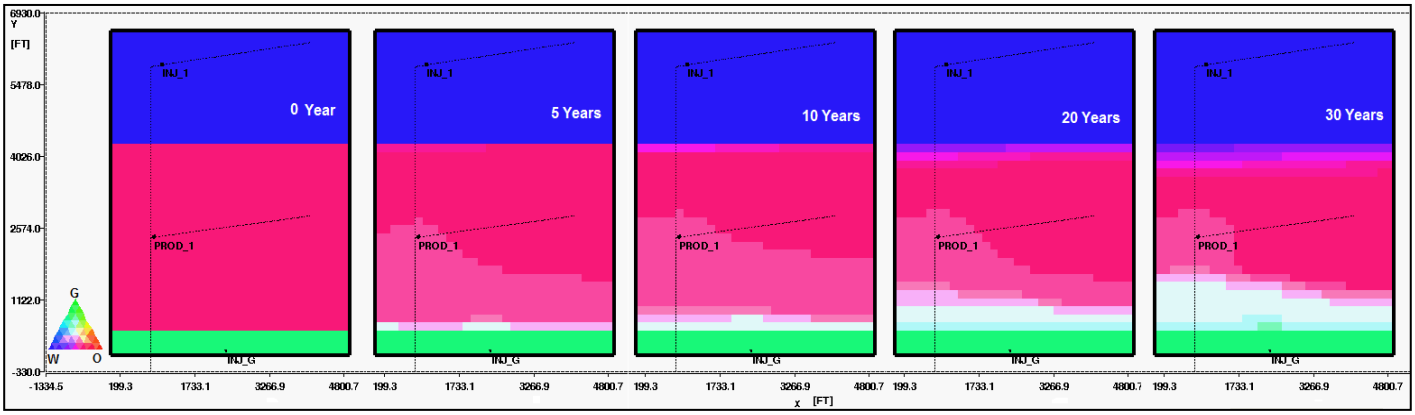

Fig.H- 1: BC cross section of saturation in the YX direction for 5 times steps for a low permeability layer of 1.05mD.

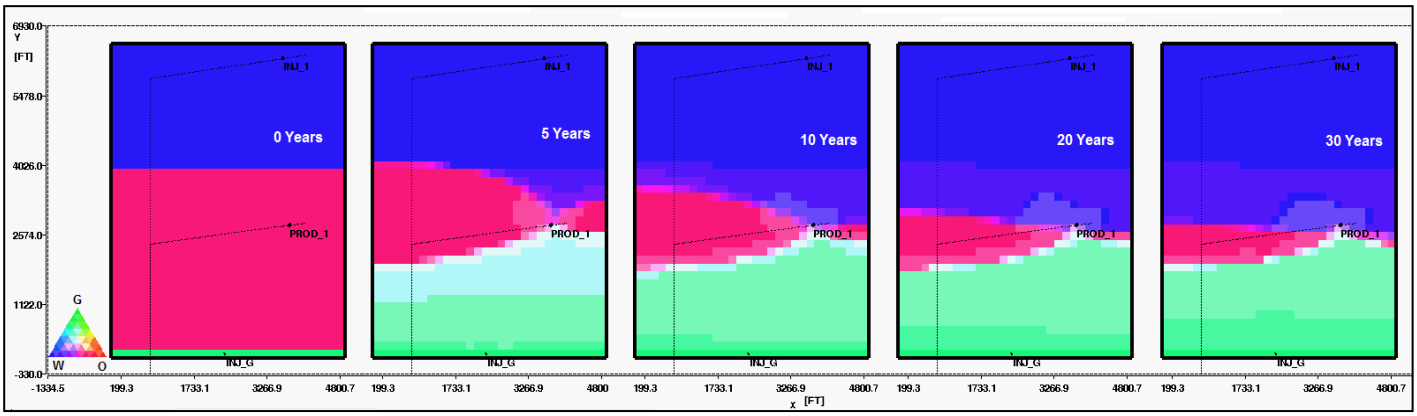

Fig.H- 2: BC cross section of saturation in the YX direction for 5 times steps for a high permeability layer of 54.35mD.

In Fig.H- 3, in BC-GCC no gas breakthrough is observed during year 1, justifying that the gas cap constraint was properly modelled.

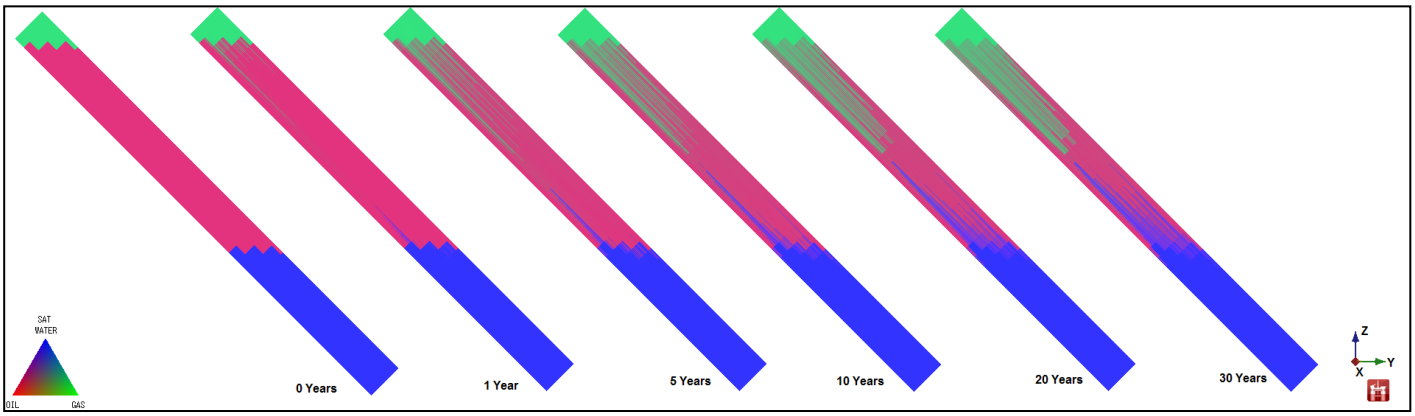

Fig.H- 3: Cross section of saturation in the ZY direction for 6 time steps of the simulation for the BC-GCC.

In Fig.H- 4 for the BC-GCC the average datum pressure is lower than in the BC, because the gas is constrained and cannot move quickly to support the pressure in the producer, which is also confirmed by the lower BHP pressure of the producer. The GOR is also lower, as gas production for this case is lower at the beginning. In both cases the water injector never reaches the BHP constraint of 6000psi.

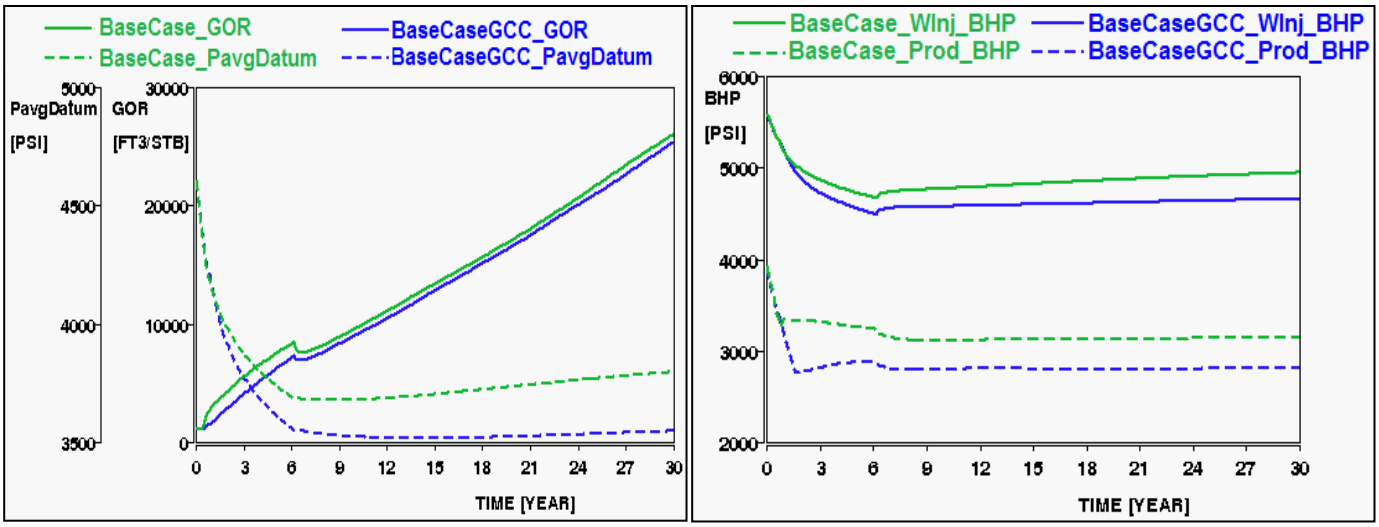

Fig.H- 4: For the Base Case and the Base Case GCC profiles of (a) Average datum pressure and GOR, (b) BHP for the water injector and the producer.

Appendix I: Simulation Results of the Sensitivity Analysis for the Cumulative Oil Production

Objective: This section presents the results of the Sensitivity Analysis for the cumulative oil production to the relative permeability data, the k_v/k_h ratio, the permeability and grid block size.

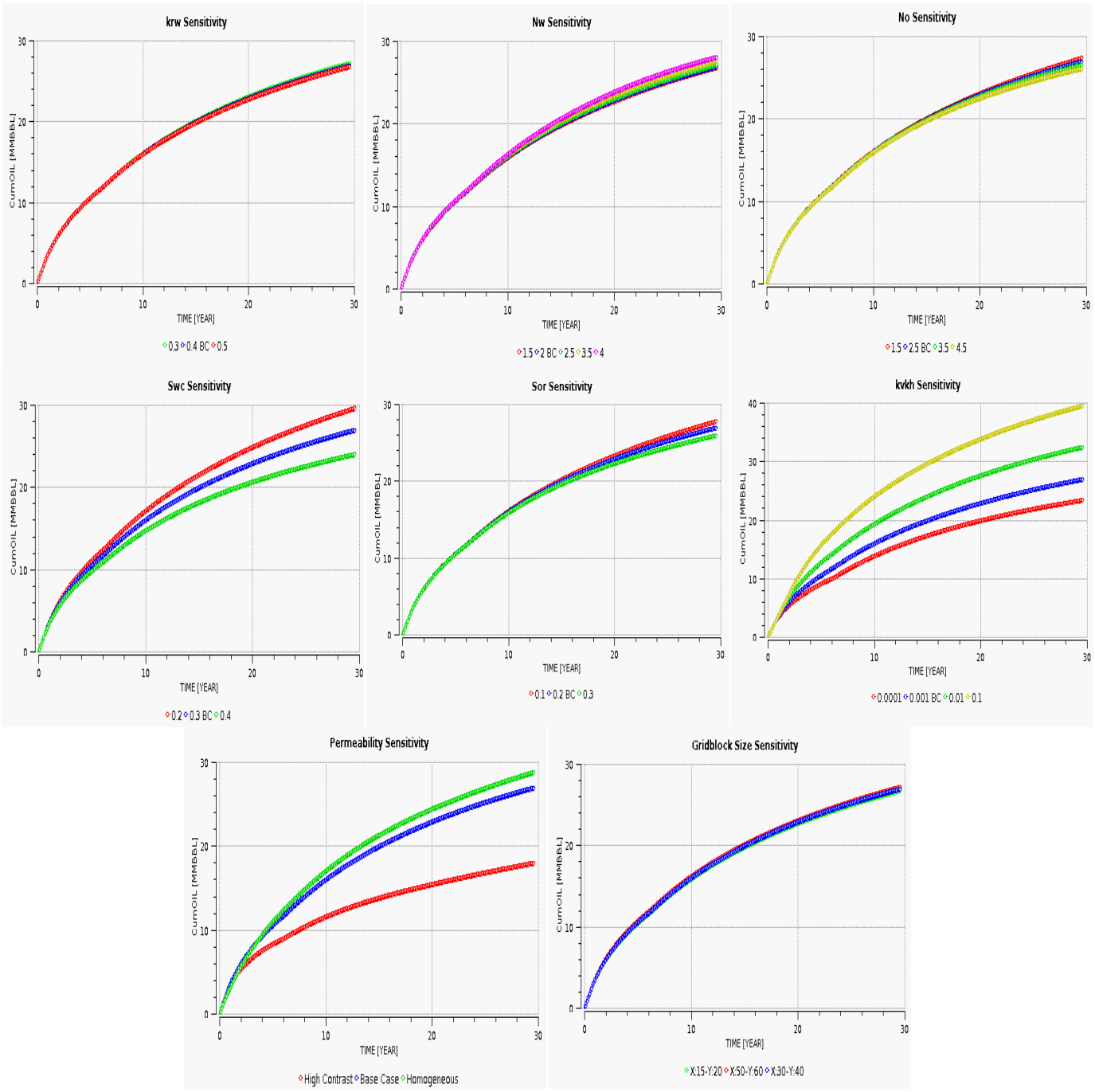

Fig.I- 1: Sensitivity analysis for cumulative oil production.

Appendix J: Simulation Results for Improvement Solutions

Objective: This section presents the results for the improved water injection, the WAG injection and the polymer flooding.

Improved Water Injection

Fig.J- 1 compares the sweep efficiency of the water injection in the case of a horizontal and a vertical well. As illustrated, with the deviated well a larger area is swept for both the high and the low permeability layers.

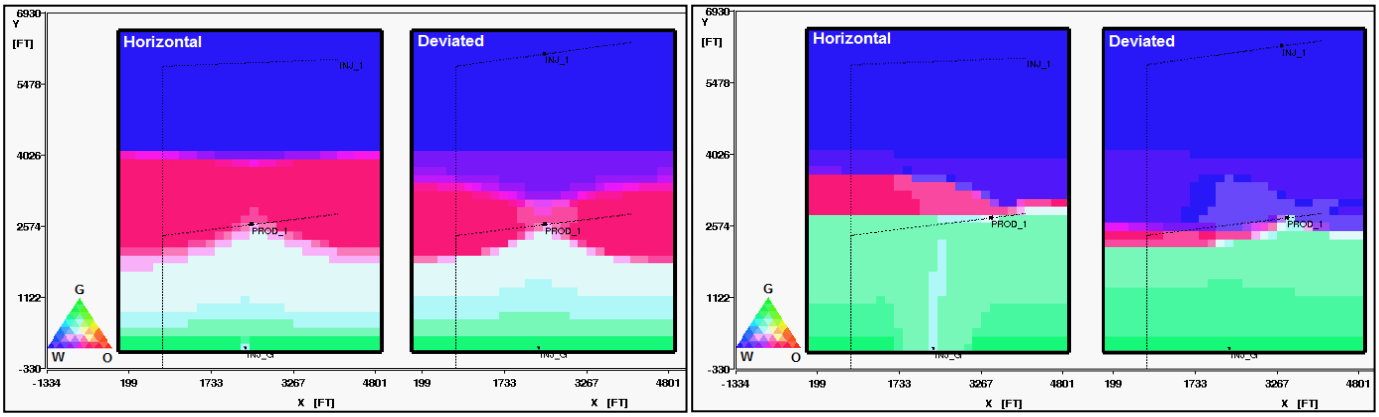

Fig.J- 1: Saturation profiles illustrating sweep, for a horizontal and a deviated well (a) for a low permeability layer of 2mD and (b) a high permeability layer of 200mD.

Fig.J- 2 compares the cumulative oil production for the BC and BC-GCC and for the selective perforation strategy. By perforating only the low permeability layers the oil production increases.

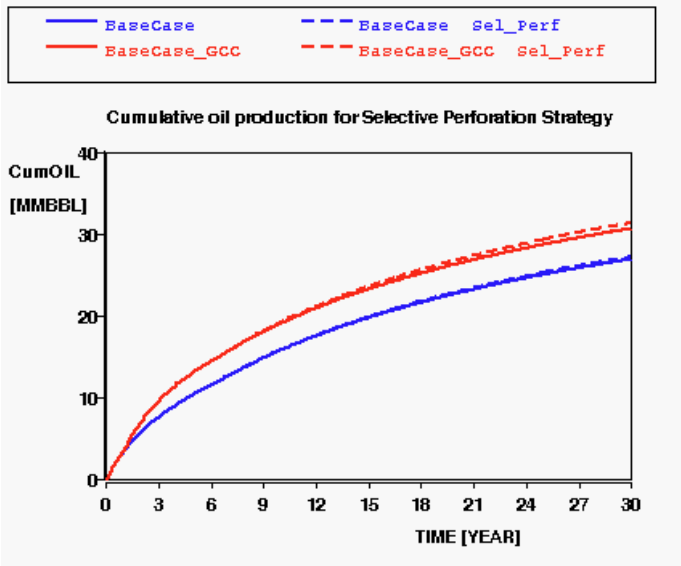

Fig.J- 2: Cumulative oil production for BC and BC_GCC using selective perforation strategy.

WAG Injection

Fig.J- 3 presents the BHP for the injector and the producer. In both cases the BHP never reaches the pressure constraint.

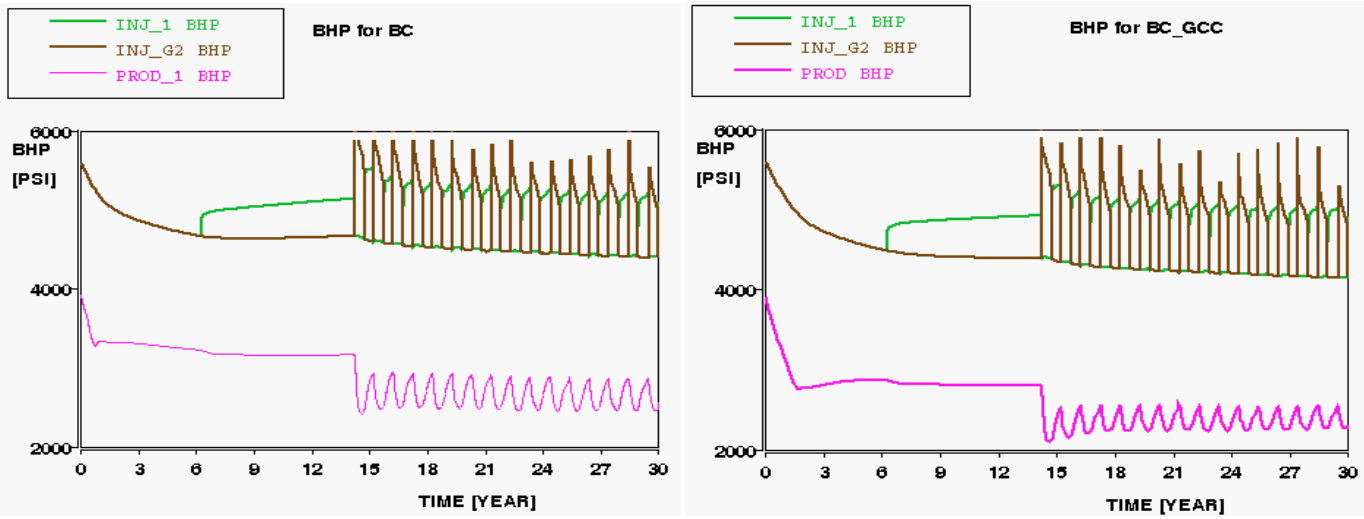

Fig.J- 3: BHP for the producer and the injector in (a) BC and (b) BC-GCC during WAG injection.

Polymer Flooding

The results for polymer flooding using a higher BHP constraint for BC are illustrated in Fig.J- 4.

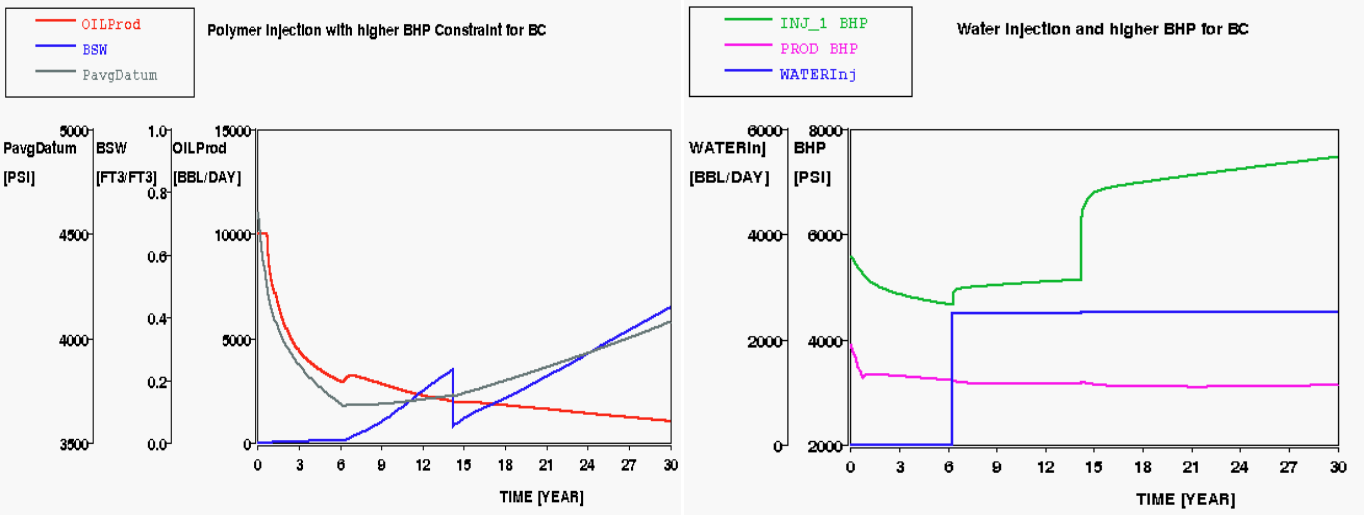

Fig.J- 4: Results for polymer flooding using higher BHP constraint for the BC.

Appendix K: Comparison of Cumulative Oil Production and Sweep Efficiency

Objective: This section presents the cumulative oil production and sweep efficiency for water, WAG and polymer injection.

Base Case

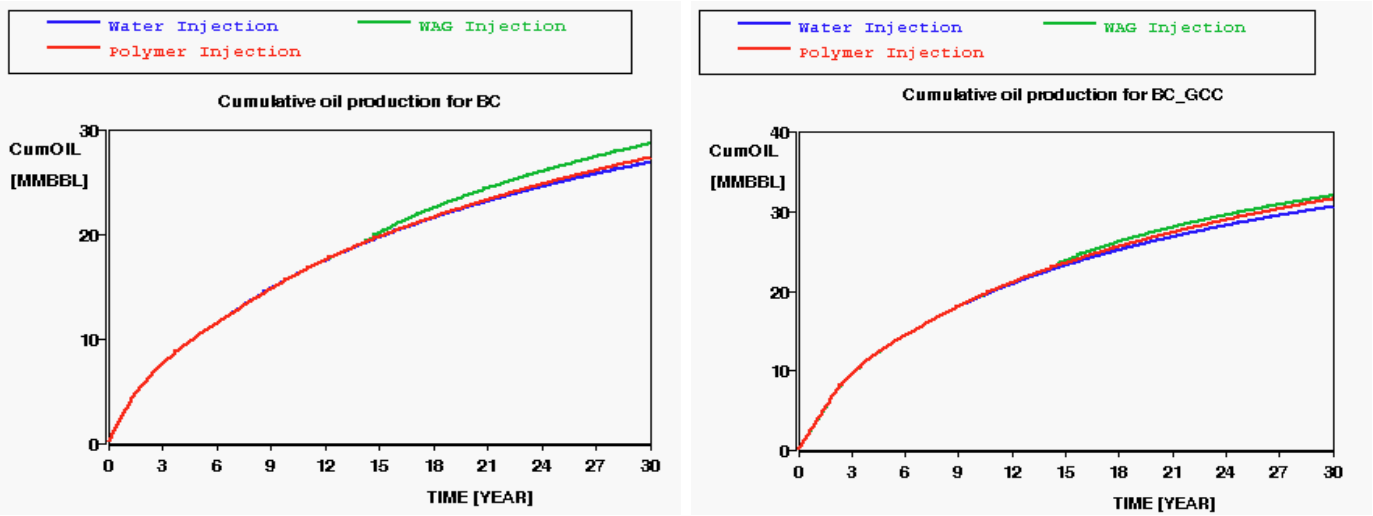

Fig.K- 1: Comparison of water, WAG and polymer injection regarding cumulative oil production for (a) BC and (b) BC_GCC.